A PERSPECTIVAL REVIEW OF RAIL BEHAVIOR AT THE FACILITY FOR ACCELERATED SERVICE TESTING

FAST Facility for Accelerated Service Testing

TRANSPORTATION TEST CENTER
PUEBLO, COLORADO 81001

PREPARED FOR
THE FAST PROGRAM

AN INTERNATIONAL GOVERNMENT - INDUSTRY RESEARCH PROGRAM

01-Track & Structures

1. Report No. FRA/TTC-81/07	2. Government Accession No.	3. Recipient's Catalog No.
4. Title and Subtitle A Perspectival Review of Rail Behavior at the Facility for Accelerated Service Testing		5. Report Date June 19, 1981
		6. Performing Organization Code
7. Author(s) Dr. R.K. Steele		8. Performing Organization Report No.
9. Performing Organization Name and Address Transportation Test Center P.O. Box 11449 Pueblo, Colorado 81001		10. Work Unit No. (TRAIS)
		11. Contract or Grant No.
12. Sponsoring Agency Name and Address U.S. Department of Transportation Federal Railroad Administration Office of Research and Development Washington, D.C. 20509		13. Type of Report and Period Covered Interim Report
		14. Sponsoring Agency Code

15. Supplementary Notes

16. Abstract

The rail metallurgy tests which have been undertaken at the Facility for Accelerated Service Testing (FAST) are described. The best of the premium metallurgies has been found to wear approximately three to four times better than standard rail in the unlubricated regime. In the lubricated regime, however, the maximum improvement in wear rate achievable by the use of a premium rail has been found to be only 50%. A strong effect of equivalent carbon has been observed for standard (Std) and high silicon (HiSi) rail in the unlubricated regime. Reduced wear and metal flow have allowed increased rail fatigue failure. When allowances are made for difference in wheel load, failure rate of Std rail at FAST is consistent with failure behavior of Std rail in U.S. railroad service. Growth of a transverse crack in the head of a rail is shown to be consistent with predictions made from simple linear elastic fracture mechanics considerations where the flexural stresses are augmented by the curving action of the train and substantial axial residual tensile stresses are assumed to exist under the work hardened running surface region of the rail head.

17. Key Words Fatigue Life Rail Metallurgy Gage Face Wear Tie Plate Cant Lubrication Transverse Crack Lubrication/Metallurgy Interaction Position-in-curve Effect		18. Distribution Statement This document is available through the National Technical Information Service 5285 Port Royal Road Springfield, Virginia 22161	
19. Security Classif. (of this report) Unclassified	20. Security Classif. (of this page) Unclassified	21. No. of Pages 56	22. Price

Form DOT F 1700.7 (8-72)   Reproduction of completed page authorized

PREFACE

This report is based upon a paper presented by R. K. Steele at the 19th Annual Conference of Metallurgists, Canadian Institute of Mining and Metallurgy in Halifax, Nova Scotia, August 26, 1980. Part of the material presented is drawn from previously issued FAST reports. However, new information on the third rail metallurgy experiment and new analyses of previous data are presented for the first time. This new information will be expanded upon in subsequent reports.

TABLE OF CONTENTS

LIST OF FIGURES

LIST OF FIGURES, CONTINUED

LIST OF TABLES

v

ACRONYMS

AAR	Association of American Railroads
AISI	American Iron and Steel Institute
AREA	American Railway Engineering Association
BSI	Boeing Services International, Inc.
FAST	Facility for Accelerated Service Testing
FHT	Fully Heat-Treated
FM	Figure of Merit
HH	Head Hardened
MGT	million gross tons
SF	Santa Fe
TD	Transverse Defect (Detail Fracture)
VHN	Vickers Hardness Number
WS	Waynesburg Southern

ABBREVIATIONS AND METRIC EQUIVALENTS

Avg	average	
CrMo	chrome molybdenum	
CrV	chrome vanadium	
HiSi	high silicon	
SiCr	silicon chromium	
Std	standard	
w/o	weight percent	
°	degree	
°F	degrees Fahrenheit	$= [(°F-32)5/9]°$ C
",in	inch	= 2.54 cm
in^2/MGT	inches per million gross tons	
kips	kilopounds	= 453.59 kg
ksi	kilopounds/$inch^2$	
mi	mile	= 1.6129 km
mi/h	miles per hour	
MGT	million gross tons	= .907 MGMg
mm	millimeters	= .04 inch
lb	pound	= .45359 kg
lb/yd	pounds per yard	
ton		= .907 metric tons
yd	yard	= .9144 m

EXECUTIVE SUMMARY

In-track studies of rail behavior conducted at the Facility for Accelerated Service Testing (FAST) at the Transportation Test Center, Pueblo, Colorado, have shown that position-in-curve effects, tie plate cant ratio, and variations in lubrication can substantially alter the conclusions drawn about wear and metal flow resistance. The best of the premium metallurgies has been found to wear approximately three to four times better than standard rail in the unlubricated regime. However in the lubricated regime, the maximum improvement wear rate achievable by the use of a premium rail has been found to be only about 50%. Wear tests of the first and second metallurgy experiments have shown that head hardened (HH) and chrome molybdenum (CrMo) rail exhibited the best overall resistance to wear and metal flow under the FAST loading environment. A 3:1 variation in gage face wear rate was found to be possible within the allowable American Railway Engineering Association (AREA) range for equivalent carbon. Reduced wear and metal flow were accompanied by increased fatigue failure of rail.

Preliminary results from the current experiment reveal that HH silicon chrome (SiCr) rail is exhibiting the best resistance to gage face wear in the unlubricated regime. Of the premium grades, the bainitic CrMo rail is wearing least well. All other premium rails--HH, 1%Cr, CrMo (weldable), chrome vanadium (CrV), and fully heat-treated (FHT)--are intermediate in behavior. In the lubricated regime, all metallurgies behave more alike, confirming the occurrence of the lubrication/metallurgy interaction. Although SiCr, 1%Cr, and CrMo (weldable) are performing equally well in Section 03, the HH and SiCr rails are wearing least in Section 17. Lubrication has been observed to have an important effect on reducing the development of welded rail end batter.

When conditions of generous lubrication have served to lengthen rail life, fatigue failure--both in the rail head and in the weldments--has become the dominant failure mode. At FAST, the fatigue failure rates of Std rail in a 5° curve and in tangent track were approximately 100 and 10 times greater, respectively, than those reported for rail in some western U.S. mainline service. When allowances are made for difference in wheel load, the failure rate of Std rail at FAST is consistent with the observed failure behavior of Std rail in some U.S. railroad service. However, the observed dependency of fatigue life on tonnage is less than that predicted by theory. The growth of a transverse crack in the rail head is shown to be consistent with predictions made from simple linear elastic fracture mechanics considerations where flexural stresses are augmented by the curving action of the train, and where substantial axial residual tensile stresses are assumed to exist under the work-hardened running surface region of the rail head.

INTRODUCTION

Ultimately, the adequacy of any rail metallurgy is judged by how well the metallurgy performs in service. This judgment will consider such factors as resistance to wear, metal flow, defect formation, and development of corrugations and welded rail end batter, along with rail straightness and weldability. However, in normal railroad service it is difficult to accumulate reliable, easily interpreted, and unbiased information about the performance of different rail metallurgies. The Facility for Accelerated Service Testing (FAST), therefore, has undertaken a series of rail metallurgy experiments over the last several years. Some of the results of these experiments will be presented and their relationship to observations from actual railroad operation will be discussed.

TEST DESCRIPTION

FAST, located at the Transportation Test Center in Pueblo, Colorado, is a 4.8 mi test loop on which a test train of 9,500 trailing tons completes up to 120 laps daily. In this way the track is subjected daily to approximately one million gross tons (MGT) of traffic. The configuration of the FAST Track is shown in figure 1. Average train speed is 41 mi/h and direction reverses daily.

In the past, two rail metallurgy experiments were conducted in Section 03 (5° curvature) and Section 13 (4° curvature). At present, a third experiment is underway in Sections 03 (5° curvature) and 17 (5° curvature, 2% grade). The physical layout of the different metallurgies in Section 03 in these three experiments is shown in figure 2. In the early experiments, the configuration of Section 13 was similar, though not identical, to Section 03. Currently, Section 17 follows the same replication scheme used in Section 03, although there are fewer metallurgies. The rails tested in Section 03 are and have been 132 lb/yd or heavier. Rail in Section 13 had been 115 lb/yd; all rail currently under test in Section 17 is 136 lb/yd. At present, rails of a given metallurgy are flash butt welded, and the different metallurgy segments are joined by glued mechanical joints. The first and second experiments included tie plate cant as a variable (1:14, 1:30, and 1:40); the standard 1:40 cant is used throughout in the third experiment.

In the first experiment, a condition of poor rail lubrication existed for the first 40 to 45 MGT; thereafter (to 135 MGT) the lubrication became very generous. Throughout the second experiment (135 to 425 MGT), a condition of very generous lubrication prevailed, reducing wear so significantly that rail fatigue became the dominant failure mode. In this third experiment, programed variations in lubrication are introduced so that wear and metal flow in both regimes can be studied. It is also hoped that this approach will more nearly equalize the wear and fatigue life of the rail.

1
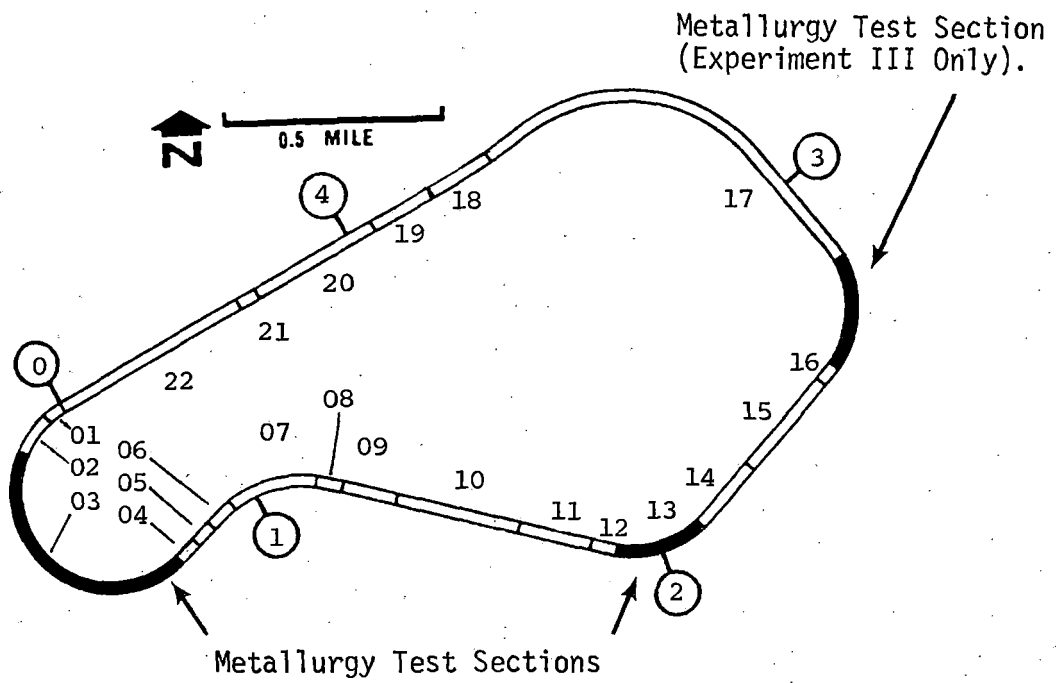
FIGURE 1. DIAGRAM OF THE FAST TRACK.

FIRST EXPERIMENT DESIGN

(Pattern in "E" Repeated in Each Segment)

Metallurgy   HH HiSi FHT CrMo Std

Segment	A	B	C	D					F	G	H	I	J
Tie Plate Cant	1:40	1:30	1:14	1:14		1:30			1:40	1:40	1:19	1:30	1:14
# Spikes/Plate	◄————————————————5————————————————►									◄—3—►	◄————5————►		

SECOND EXPERIMENT DESIGN

Metallurgy	Std	HH	CrMo	FHT	HiSi	Std	HH	CrMo	FHT	HiSi	Std	HH	CrMo	FHT	HiSi
Tie Plate Cant	1:40		1:30		1:14		1:40		1:30			1:14			1:40

All Segments Have 5 Spikes/Plate.

THIRD EXPERIMENT DESIGN

Std	HH	CrMo1	SiCr	1%Cr	CrMo2	HH	Std	FHT	HH	STD	CrMo1	SiCr	1%Cr	CrMo2	Std	HH

Cant Is 1:40 Throughout.   All Segments Have 5 Spikes/Plate.

CrMo1 = Bainitic   CrMo2 = Weldable

FIGURE 2.   LAYOUT OF METALLURGIES IN SECTION 03.

3

MATERIALS

The average or nominal compositions of the rails tested for these experiments are given in table 1. About ten different heats each of standard (Std) and high silicon (HiSi) rails were tested in the first experiment. In the current experiment, the chrome molybdenum (CrMo) and chrome vanadium (CrV) are from two different manufacturers and the 1%Cr (1Cr) has been supplied by three different manufacturers. The CrMo rail is of two different types--a partially bainitic grade and a weldable grade that requires no post-heat after flash butt welding.

TABLE 1. AVERAGE CHEMICAL ANALYSES OF RAIL IN THE FAST
METALLURGY EXPERIMENTS.

Rail Type	Weight Per Cent, (w/o)							
	C	Mn	P	S	SI	Cr	Mo	V
Section 03 (>132 lb/yd)								
Std	0.78	0.86	0.027	0.025	0.15	--	--	--
HISI	0.76	0.86	0.028	0.027	0.63	--	--	--
FHT	0.69	0.81	0.018	0.032	0.18	--	--	--
CrMo	0.80	0.82	0.026	0.025	0.25	0.78	0.20	--
HH	0.79	0.84	0.009	0.018	0.16	--	--	--
Section 13 (115 lb/yd)								
Std	0.73	0.86	0.024	0.020	0.17	--	--	--
HISI	0.77	0.88	0.029	0.024	0.68	--	--	--
FHT	0.77	0.81	0.020	0.041	0.15	--	--	--
HH	0.77	0.88	0.015	0.025	0.18	--	--	--
Sections 03 and 17								
(FHT, HH Analyses not available at this time)								
(132,136, 140 lb/yd) CrMo1*	0.72	0.79	0.009	0.023	0.25	0.78	0.21	
CrMo2	0.70/0.80	0.50/0.70	0.030 max	0.025 max	0.20/0.25	0.50/0.70	0.16/0.20	
1Cr (a)	0.71	0.73	0.014	0.021	0.27	1.16	--	--
(b)	0.73	1.30	0.023	0.026	0.30	1.25	--	--
(c)	0.75	0.88	0.030	0.027	0.23	0.95	--	--
CrV (d)	0.72	1.27	0.014	0.03	0.22	1.04	--	0.087
(e)	0.67	1.15	0.009	0.013	0.34	1.11	--	0.11
CrSI(HH)	0.76	0.82	0.020	0.006	0.82	0.50	--	--
Std	0.76	0.86	0.022	0.024	0.18	--	--	--

*CrMo1 = Balnitic   1Cr (a,b,c): 1Cr, 3 different manufacturers;
CrMo2 = Weldable   CrV (d,e): CrV, 2 different manufacturers;
see text: Materials.

4

RESULTS AND DISCUSSION

WEAR AND METAL FLOW

The chief parameter studied has been curve wear on the high rail. The measures of this wear are: gage face wear, head height loss, and total head area change. In addition, head height loss and lateral metal flow are measured on the low rail. All of these measurements are illustrated in figure 3. In the first and second experiments, the measurements were taken from profiles obtained by rather inexact ($\pm$ 0.020") profilometry techniques, thus reducing the strength of the conclusions to be drawn, particularly in the second experiment where the wear rates were low. In the current experiment, some wear measures are obtained with direct reading instruments (snap gages) of much greater sensitivity ($\pm$ 0.002"). Typical scatter of data for each method is shown in figures 4 and 5 (which, respectively, represent measurements from the first and third experiments).

High rail wear rates were determined by regression fitting the data from the first experiment to a linear wear model of the form:

$$W = W_o + \alpha MGT_I + \beta MGT_{II} + \ldots$$

where:

W = the measure of wear,

W_o = indicated wear at zero MGT,

α = the wear rate in first (I) regime of lubrication,

β = the wear rate differential in the second (II) regime of lubrication, and

$MGT_{I,II}$ = the tonnage in each regime of lubrication.

Analyses of variance and covariance were applied to groupings of the data, as well as to the entire body of data, to test the conclusions for statistical significance.

Generally, the results from the first experiment, in the more poorly lubricated regime, may be summarized as follows (see tables 2 through 8):

- CrMo and HH rail exhibited the greatest resistance to gage face wear and head area loss.

- HiSi and FHT rails were significantly less resistant to gage face wear and head area loss, although FHT rail exhibited somewhat better resistance to head height loss than did HH rail.

- The 1:14 tie plate cant produced approximately 20% more gage face wear and head area loss, on the average, for all metallurgies than did either the

5

Gage Face Width ┄┄┄┄Head Height

5/8"

10° | 10°

Width To
Gage Side
Flow Lip

Width To
Field Side
Flow Lip

Total Area Within
Shaded Boundary
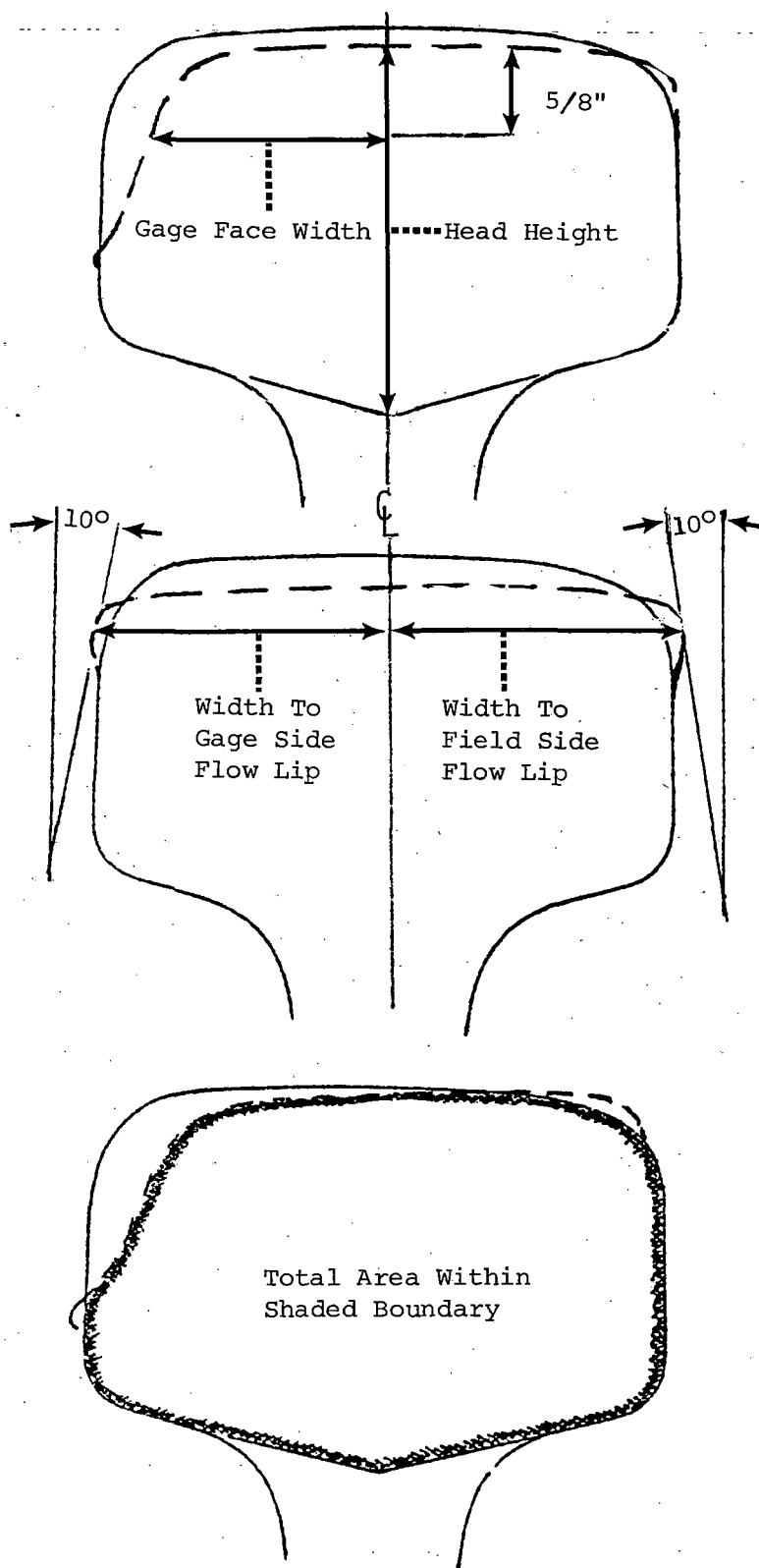
FIGURE 3. RAIL HEAD DIMENSIONS AND AREAS.
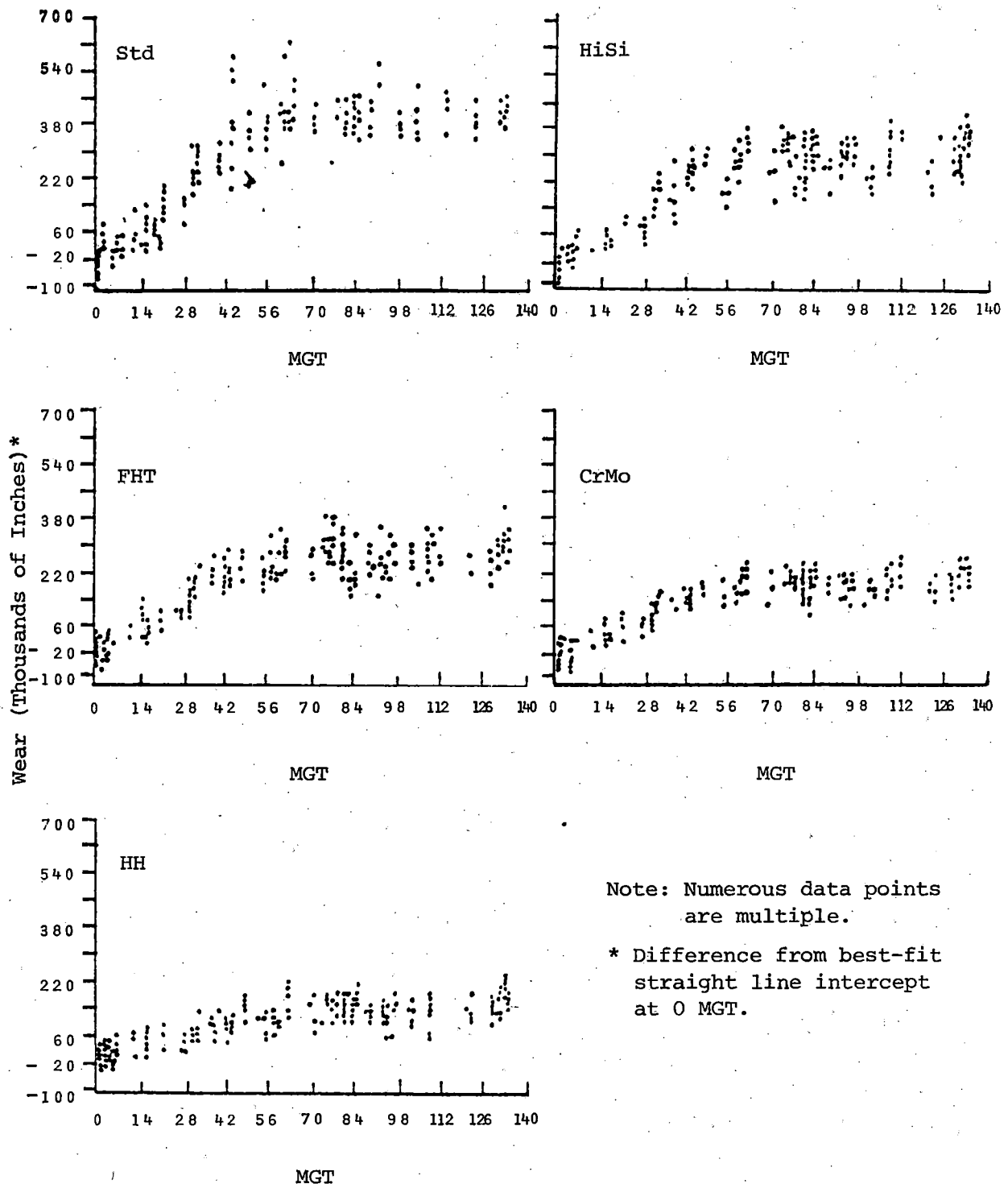
FIGURE 4. PROFILOMETER MEASUREMENTS (FIRST EXPERIMENT), GAGE FACE WEAR,*
ALL FIVE METALLURGIES ON 1:40 CANT TIE PLATES, SECTION 03.
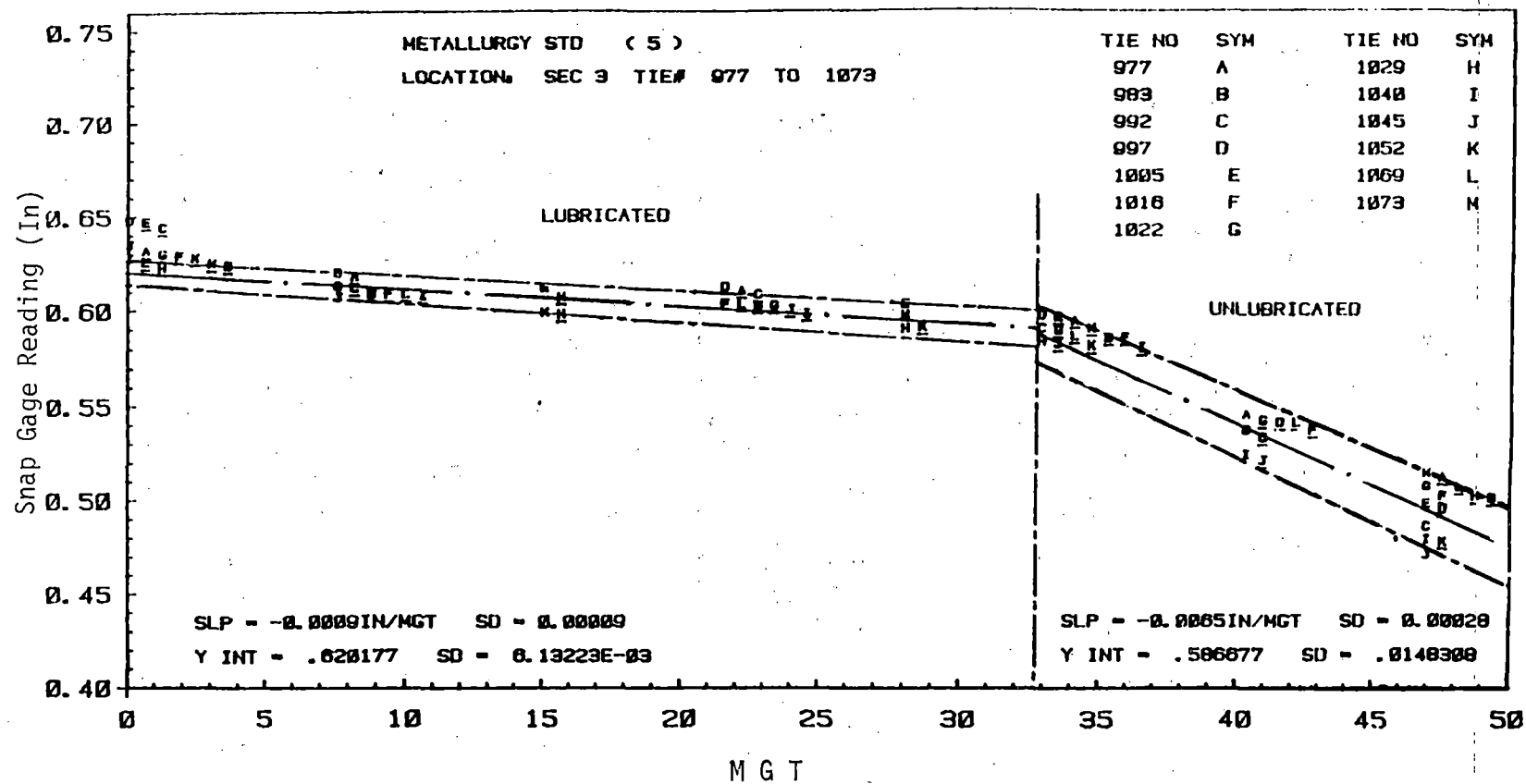
FIGURE 5. SNAP GAGE MEASUREMENTS (THIRD EXPERIMENT) OF STD RAIL
           IN SECTION 03, TIES 0977 TO 1073.

TABLE 2. WEAR RATES ABOVE AND BELOW THE LUBRICATION TRANSITION
FOR THE DIFFERENT TIE PLATE CANTS, SECTION 03.

Tie Plate Cant

	Metallurgy	1:40		1:14		1:30	
		Below	Above	Below	Above	Below	Above
Gage Face Loss (in/MGT)	HH	0.00271	0.00030	0.00384	0.00090	0.00298	0.00054
	HiSi	0.00579	0.00031	0.00707	0.00149	0.00513	0.00097
	FHT	0.00550	0.00082	0.00658	0.00111	0.00548	0.00102
	CrMo	0.00355	0.00059	0.00444	0.00111	0.00401	0.00097
	Std	0.00809	0.00072	0.00835	0.00135	0.00778	0.00099
Head Area Loss (in^2/MGT)	HH	0.00496	0.00046	0.00514	0.00092	0.00424	0.00097
	HiSi	0.00812	0.00110	0.00907	0.00119	0.00708	0.00154
	FHT	0.00704	0.00046	0.00667	0.00149	0.00627	0.00183
	CrMo	0.00449	0.00092	0.00423	0.00107	0.00482	0.00085
	Std	0.01287	0.00167	0.01245	0.00127	0.01229	0.00156
Head Height Loss (in/MGT)	HH	0.00127	*	0.00109	*	0.00090	*
	HiSi	0.00144	*	0.00134	*	0.00122	*
	FHT	0.00097	*	0.00056	0.00005	0.00079	*
	CrMo	0.00073	*	0.00053	*	0.00052	0.00006
	Std	0.00256	0.00001	0.00233	0.00011	0.00223	0.00030

Note:
Wear rates were determined from analysis of covariance of all
metallurgies together.
* Indicates no significant wear.

TABLE 3. AVERAGE GAGE FACE LOSS RATE FOR ALL CANTS, SECTION 03.

	Below Lubrication Transition		Above Lubrication Transition	
	Gage face loss (in/MGT)	FM*	Rate (in/MGT)	FM
Std	0.0086	1	0.0012	1
HiSi	0.0061	1.4	0.0012	1
FHT	0.0059	1.5	0.0011	1.1
CrMo	0.0041	2.1	0.0011	1.1
HH	0.0032	2.7	0.0007	1.5

*FM = Figure of Merit = $\dfrac{\text{Average Wear Rate of Std Rail}}{\text{Average Wear Rate of Premium Rail}}$

TABLE 4. TIE PLATE CANT EFFECT ON GAGE FACE WEAR RATE IN SECTION 03.

Tie Plate Cant	Below Lubrication Transition Rate (in/MGT)	Above Lubrication Transition Rate (in/MGT)
1:40	0.0053	0.0008
1:30	0.0053	0.0011
1:14	0.0062	0.0013

TABLE 5. POSITION-IN-CURVE EFFECT ON GAGE FACE WEAR RATE IN SECTION 03.

Position-in-curve	Below Lubrication Transition Rate (in/MGT)	Above Lubrication Transition Rate (in/MGT)
Section 02 End	0.0052	0.0012
Middle, Section 03	0.0054	0.0017
Section 04 End	0.0064	0.0006

TABLE 6.   GAGE FACE WEAR RATE RESULTS, SECTION 13 (FIRST EXPERIMENT).

Metallurgy Below Transition	Position in Curve* Wear Rate (in/MGT)					Average Figure of Merit
	A	B	C	D	Avg	
HH	0.0021	0.0017	0.0025	0.0021	0.0022	3.5
HiSi	0.0052	0.0049	0.0045	0.0043	0.0047	1.6
FHT	0.0038	0.0038	0.0034	0.0037	0.0037	2.1
Std	0.0063	0.0092	0.0094	0.0060	0.0077	1.0
Avg	0.0044	0.0049	0.0050	0.0046		
Above Transition						
HH	0.0014	0.0012	0.0003	0.0010	0.0010	1.3
HiSi	0.0025	0.0001	0.0006	0.0014	0.0012	1.1
FHT	0.0020	-0.0001	0.0010	0.0012	0.0010	1.3
Std	0.0016	0.0010	0.0010	0.0016	0.0013	1.0
Avg	0.0019	0.0006	0.0007	0.0013		

* Section 13:

    A   = Section 12 End, Section 13
    B,C = Middle, Section 13
    D   = Section 14 End, Section 13

11

TABLE 7.   COMPARISON OF GAGE FACE WEAR RATES IN SECTIONS
03 AND 13, ALL ON 1:40 TIE PLATE CANT.

Metallurgy	Section 03 (5°)				Section 13 (4°)			
	Below Transition		Above Transition		Below Transition		Above Transistion	
	Wear Rate (In/MGT)	FM	Wear Rate (In/MGT)	FM	Wear Rate (In/MGT)	FM	Wear Rate (In/MGT)	FM
Std	0.0097	1.0	0.0016	1.0	0.0077	1.0	0.0013	1.0
HiSi	0.0063	1.5	0.0013	1.2	0.0047	1.6	0.0012	1.1
FHT	0.0060	1.6	0.0012	1.3	0.0037	2.1	0.0010	1.3
HH	0.0026	3.7	0.0010	1.6	0.0022	3.5	0.0010	1.3

Note:
    Wear rates were determined by regression on each metallurgy data set independently.

TABLE 8.   RATIO OF GAGE FACE WEAR RATE IN SECTIONS 03 AND 13.

Ratio: $\dfrac{\text{Wear Rate (in/MGT) Section 13}}{\text{Wear RAte (in/MGT) Section 03}}$

Metallurgy	Below Transition	Above Transition
Std	0.804	0.906
HiSi	0.746	0.671
FHT	0.617	0.809
HH	0.846	0.993
Average *	0.753	0.845

* Overall Average = 0.799

12

1:30 or 1:40 cant plate, although the 1:40 cant plate caused slightly more head height loss.

- However, for Std rail alone, the gage face wear rate and head area loss rates were so high there really was no difference in these parameters for any of the tie plate cants.

When lubrication improved after 40 to 45 MGT, the wear behavior changed with somewhat unexpected results:

- A strong metallurgy:lubrication interaction was observed as a reduction in the wear resistance benefit of premium rails relative to Std rail; i.e., all metallurgies looked more alike.

- The strength of the tie plate cant diminished significantly, but the 1:40 cant consistently evidenced the lowest gage face and head area loss.

However, it should be pointed out that the purpose of using 1:14 cant tie plates was not to alter wear behavior, but rather to redistribute the location of wheel/rail contact so as to reduce shell and detail fracture occurrence; more will be said about this later.

The position-in-curve effect led to an approximate 20% variation in gage face wear through the curve in the underlubricated regime. However, when lubrication improved, the relative position-in-curve variability appeared to increase significantly; variations in average gage face wear rate from one position to another in the curve were sometimes much greater than the variations from one metallurgy to another.

Wear behavior of the different metallurgies in the 4° curve (Section 13) was basically the same as that observed in the 5° curve (Section 03), see table 7. Overall (and irrespective of the amount of lubrication), the wear rate for any given metallurgy in the 4° curve was less by about 20% than that in the 5° curve, which is consistent with a linear relationship between wear and curvature. However, if each metallurgy is examined individually, the ratio between 4° curve wear and 5° curve wear can vary from 0.617 (FHT, poor lubrication) to 0.993 (HH, well-lubricated), see table 8. However, this conclusion is confounded somewhat by the fact that the 4° curve had all 115 lb/yd rail, while the 5° curve had both 132 and 136 lb/yd rail.

Preliminary results from the second experiment, given in table 9, indicate that, basically, the metallurgies behaved the same as they did in the well-lubricated regime of the first experiment. However, CrMo appeared to perform substantially better than did HH, primarily because of the apparent difference in behavior in the Section 02 end of the Section 03 curve. Statistical analysis of these preliminary results showed no tie plate cant effect. Also, the position-in-curve effect was weak (significant only at 95% confidence). The gage face wear rates in the second experiment were substantially less than those under comparable lubrication conditions in the first experiment (table 10).

Before examining the first results from the current experiment, it will be useful to examine the results from the first experiment in greater detail.

13

TABLE 9. PRELIMINARY GAGE FACE WEAR RESULTS (IN/MGT)
FROM THE SECOND METALLURGY EXPERIMENT, SECTION 03.

| Metallurgy | Position | | | Average* (in/MGT) | FM |
	Section 02 End of Section 03 (in/MGT)	Middle of Section 03 (in/MGT)	Section 04 End of Section 03 (in/MGT)		
Std	0.0006	0.0007	0.0005	0.0006	1
HH	0.0004	0.0003	0.0002	0.0003	2
CrMo	0.0001	0.0002	0.0002	0.0002	3
FHT	0.0005	0.0006	0.0005	0.0005	1.2
HiSi	0.0006	0.0007	0.0005	0.0006	1

* Rounded off

TABLE 10. COMPARISON OF WEAR RATES, SECTION 03, SHOWING
POSITION IN CURVE EFFECTS.

| Location | Wear Rates * (in/MGT) | |
	First Experiment	Second Experiment
Section 02 End	0.0012	0.00045
Middle	0.0017	0.00049
Section 04 End	0.0006	0.00037

* Average of all metallurgies on all cants in lubricated regime.

In terms of the relationship between total gage face wear and wear on the running surface (head height loss), figure 6 shows that each metallurgy behaved differently. Std and HH rail behaved very much alike and the ratio of gage face to head height loss was only slightly reduced by lower tie plate cant. But the relative gage face/head height wear rates of CrMo and FHT rails exhibited a great dependence upon tie plate cant. Thus, the overall wear behavior appears to have depended upon a metallurgy/cant interaction as well.

If the Std and HiSi gage face wear rates from the underlubricated regime of the first experiment are corrected for tie plate cant and position-in-curve effects, the influence of chemical composition on wear rate can be determined. Using the relationship for equivalent carbon proposed by Clayton[1] with ladle analysis, figure 7 shows that within the allowable AREA composition range for Std carbon rail, a 3:1 variation in gage face wear rate can occur on a 5° curve. This magnitude of variation was as great as that observed for the difference between the average Std rail and the best premium rail, which may suggest that a relatively inexpensive way to obtain improved curve wear life is to segregate rail that is at the high end of the AREA composition range for curve use.

Rail wear in the unlubricated regime was substantially greater at FAST than that reported for typical U.S. service. This trend is reflected in figure 8 where the data of Rougas,[2] and Hay, et al.,[3] fall well below the FAST data for 5° curvature. Even the data of Stone[4] for the Waynesburg Southern (WS), with 125-ton cars, fall below the FAST data for standard rail at 5° curvature. However, the data of Curcio, et al.,[5] for Std rail at 2° and 3° of curvature, lie close to a straight line that would join the FAST Std rail data point (in the underlubricated regime) with zero wear at zero MGT. Although Curcio, et al., report that lubrication was applied at the entry of the test curves, information about lubrication for the other data sets is not reported.

A typical set of gage face wear data from the third experiment determined from direct dial (snap) gage measurements is shown in figure 5. The wear rate averages from Section 03 and 17 are tabulated in tables 11 and 12. Again, a

---

[1] Clayton, P., "The Relationships Between Wear Behavior and Basic Material Properties for Pearlitic Steels," Wear of Materials 1979, American Society of Mechanical Engineers, New York, N.Y., pp 35-44.

[2] Rougas, M., 1975 Technical Proceedings of the 12th Annual Railroad Engineering Conference, Report No. FRA-OR&D-76-243, October 1975, pp 41-44.

[3] Hay, W.W.; Reinschmidt, A.J.; Bakas, P.T.; and Schuch, P.M., Economic Evaluation of Special Metallurgy Rails, Report No. ENG-76-2002, University of Illinois at Urbana-Champaign, Urbana, IL, January, 1976, NTIS #PB 252 024.

[4] Stone, D.H., Comparison of Rail Behavior with 125-Ton and 100-Ton Cars, Report No. R-405, Association of American Railroads, Chicago, IL, January, 1980.

[5] Curcio, P.; Marich, S.; and Nisich, G., "Performance of High Strength Rails in Track," Paper I.10, Heavy Haul Railways Conference, Perth, Western Australia, September, 1978.

FIGURE 6. VARIATION IN RATIO OF WEAR RATES WITH METALLURGY
AND TIE PLATE CANT.

16

Gage Face Wear Rate (0.001 in/MGT) vs Equivalent Carbon $^W/_0$

$$c_{eq} = w/o\,C + \frac{w/o\,Mn}{4.75} + \frac{w/o\ Si}{10}$$

$3.8 \times 10^{-3} - 3.1 \times 10^{-3}\ c_{eq}$
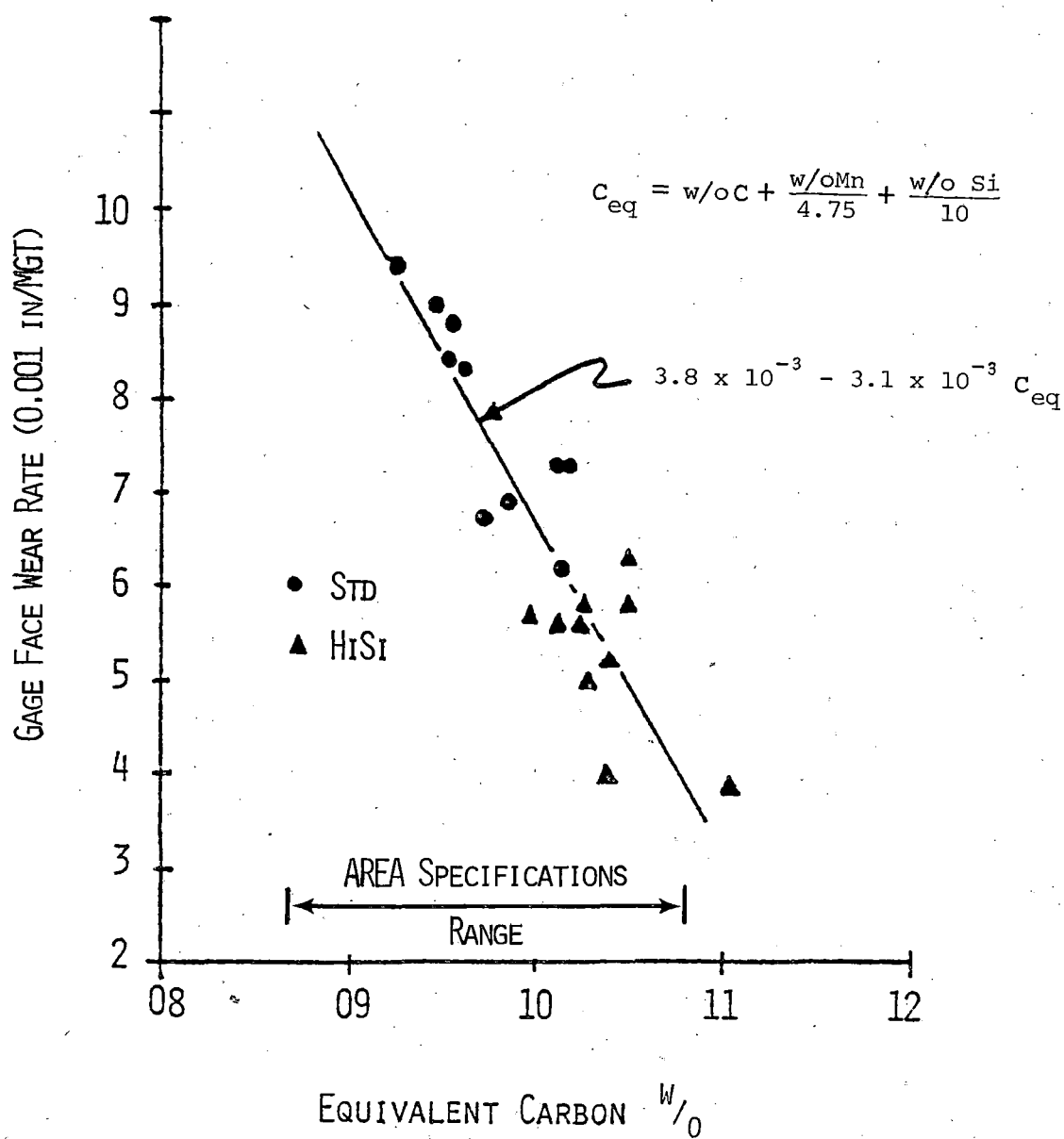
● STD
▲ HiSi

AREA Specifications
Range

FIGURE 7. EFFECT OF EQUIVALENT CARBON LEVEL ON GAGE FACE WEAR RATE.
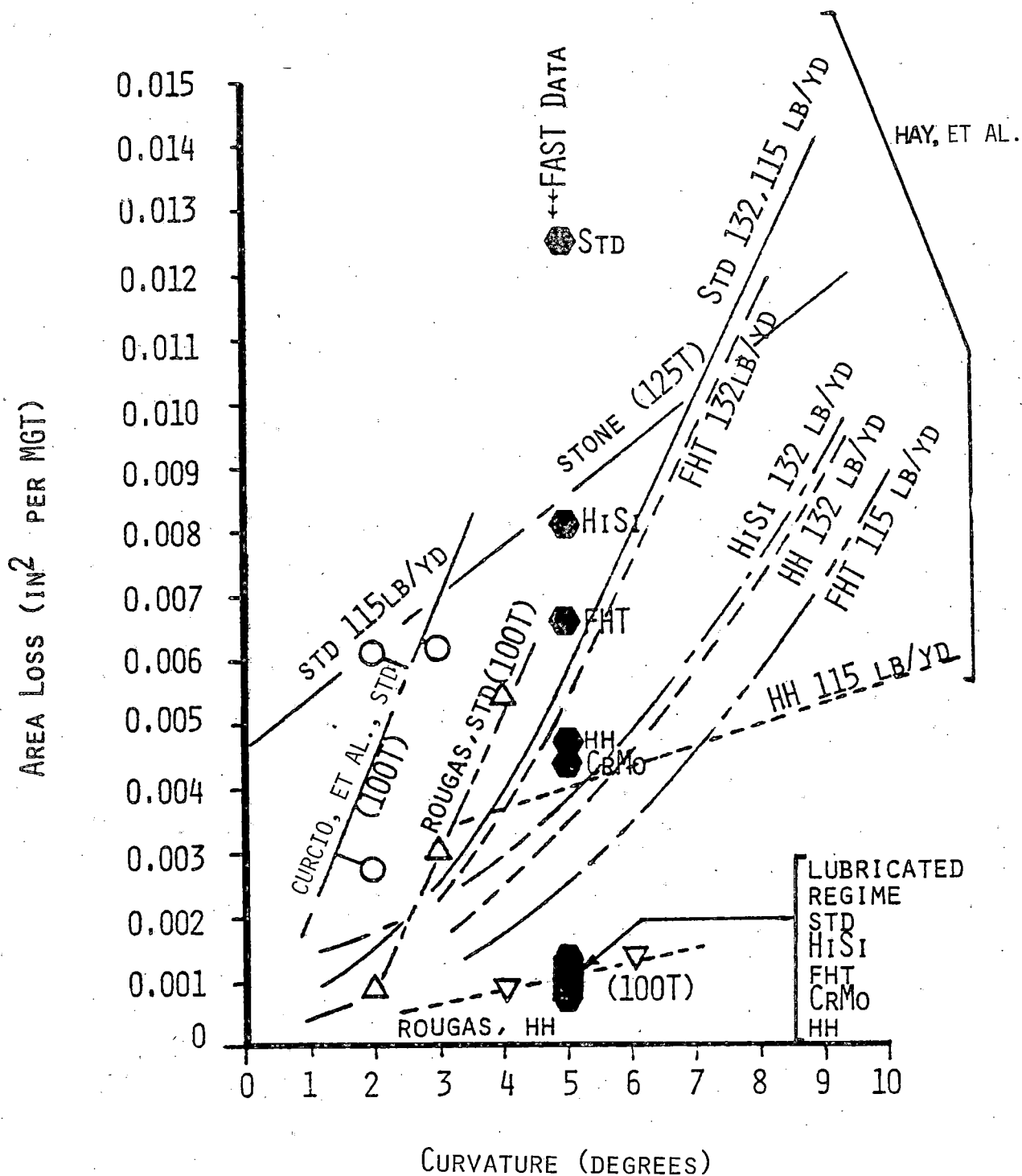
17

FIGURE 8.   COMPARISON OF WEAR RATE DATA.

TABLE 11. GAGE FACE WEAR RATES FROM THE THIRD METALLURGY EXPERIMENT, SECTION 03.

| Metallurgy/Tie range | Wear Rates (in/MGT) | | | |
	Lubricated Wear rate	Avg Wear rate	Unlubricated Wear rate	Avg Wear rate
Std				
Tie # 110 to 200	0.0010		0.0059	
Tie # 977 to 1429	0.0009	0.0010	0.0065	0.0066
Tie # 1358 to 1429	0.0011		0.0069	
Tie # 1955 to 2040	0.0011		0.0069	
HH Std				
Tie # 220 to 314	0.0006		0.0020	
Tie # 865 to 954	0.0008	0.0008	0.0024	0.0023
Tie # 1217 to 1314	0.0007		0.0027	
Tie # 2086 to 2177	0.0009		0.0021	
HH SiCr				
Tie # 475 to 554	0.0007		0.0016	
Tie # 1591 to 1669	0.0006	0.0007	0.0019	0.0017
1%Cr				
Tie # 600 to 707	0.0006		0.0027	
Tie # 1716 to 1801	0.0007	0.0007	0.0031	0.0029
CrMo (Weldable Grade)				
Tie # 751 to 830	0.0006		0.0028	
Tie # 1841 to 1919	0.0007	0.0007	0.0031	0.0029
CrMo (Bainitic)				
Tie # 354 to 428	0.0009		0.0039	
Tie # 1470 to 1544	0.0009	0.0009	0.0033	0.0036
FHT				
Tie # 1096 to 1190	0.0007	-	0.0031	

TABLE 12. GAGE FACE WEAR RATES FROM THE THIRD METALLURGY EXPERIMENT,
          SECTION 17.

| Metallurgy/Tie Range | Wear Rates (in/MGT) | | | |
	Lubricated	Avg	Unlubricated	Avg
HH Std				
Tie # 494 to 555	0.0003		0.0023	
HH SiCr				
Tie # 138 to 226	0.0003		0.0015	
Tie # 592 to 678	0.0003	0.0003	0.0016	0.0016
1%Cr				
Tie # 382 to 454	0.0002		0.0028	
Tie # 820 to 905	0.0005	0.0003	0.0031	0.0030
CrV				
Tie # 261 to 330	0.0003		0.0032	
Tie # 716 to 770	0.0005	0.0004	0.0024	0.0027

lubrication/metallurgy interaction is observed. This is exemplified by the
fact that the figure of merit (FM) of SiCr rail (relative to Std rail) is
about 3.9 in the dry regime, but only about 1.5 in the lubricated regime.
Although considerable differences in wear rate exist among the premium
metallurgies in the dry regime, in the lubricated regime most behaved very
much alike. An exception seems to be the bainitic CrMo, which (in the lubri-
cated regime) wore virtually the same as did Std rail. In the dry regime,
head hardened SiCr rail exhibited the greatest resistance to gage face wear,
followed in descending order by HH, 1Cr and CrMo (weldable), CrV, FHT, and
(finally) bainitic CrMo. In the lubricated regime, HH wore very slightly more
than SiCr, 1Cr, and CrMo (weldable) in Section 03. In Section 17
(lubricated), the HH and SiCr exhibited the lowest wear rate.

It is not clear why a lubrication/metallurgy interaction should exist, but
the implication is that lubrication has a greater affect on Std rail than it
does on premium rails. Jamison,[6] in offering an explanation of humidity
effects in the wear process, has suggested a wear model which could explain
the lubrication/metallurgy interaction. The theory suggests that increased
friction (lack of lubrication) tends to bring the subsurface plastic zone to
the surface. This effect will be more pronounced in the lower strength rail
and, therefore, the wear of Std rail will be more influenced by lack of lubri-
cation than will that of the premium rails.

-----
[6] Jamison, W.E., "Wear of Steel in Combined Rolling and Sliding," ASME/ASLE Lubrication
     Conference, San Francisco, CA, August 18-21, 1980.

20

In the dry regime, the wear rates of a given metallurgy in Sections 03 and 17 are nearly identical, but in the lubricated regime, the wear rate of a given metallurgy in Section 17 may be only one-half what it is in Section 03. This difference suggests the existence of a section/lubrication interaction.

In the underlubricated regime (with the exception of the bainitic CrMo), the wear rates in the more northerly (Section 02 end) third of Section 03 appeared to be 10% to 15% less than those in the remainder of the curve. This behavior was similar, although less sharply defined, to that observed in the more poorly lubricated regime of the first experiment. The substantial position-in-curve effect observed in the lubricated regime of the first experiment has not been repeated in the initial part of this third experiment.

Table 13 shows the wear rates of Std and HH rail in each of the experiments (for each lubrication regime) together with the wheel-mix used. In both the lubricated and nonlubricated regimes, the modest reduction in rail wear rate from the first to the third experiment has accompanied an increase in the proportion of class C (harder) wheels used. Both Marich and Curcio,[7] and Babb and Lee[8] have cited laboratory studies to suggest that harder wheels may cause less rail wear; the data contained in table 13 seem to support these observations. However, other laboratory studies by Kumar and

TABLE 13. RELATIONSHIP OF WHEEL MIX AND GAGE
FACE WEAR RATES IN SECTION 03.

Experiment	Poor Lube Period					Generous Lube Period				
	Wheel Mix %			Rail Wear(in/MGT)		Wheel Mix %			Rail Wear(in/MGT)	
	B	C	U	Std	HH	B	C	U	Std	HH
I	4	32	64	0.0086	0.0032	9 7*	43 38*	48 55*	0.0012	0.0008
II	--	--	--	--	--	7	60	33	0.0006	0.0003
III	0	45	55	0.0066	0.0023	0	78	22	0.0010	0.0008

* For 2/3 of period.

B = Class B wheels
C = Class C wheels
U = Untreated wheels

-----

[7] Marich, S., and Curcio, P., MRL Report/083/76/015, Broken Hill Proprietary Co., Melbourne, Australia.

[8] Babb, A.S., and Lee, J., Fourth International Wheelset Congress, July 1972, pp. 16-30.

Margasahayam[9] and Jamison[10] show increased rail wear with the use of harder wheel steels, and vice versa. In any event, the FAST data show that modest increases in the proportion of class C wheels used did not produce a detectable increase in rail wear rates. It is not clear why the preliminary wear data from the second experiment differ from those of the lubricated portions of the first and third experiments.

As shown in figure 9, premium metallurgy average head area loss FM from the first experiment appear to observe two separate linear dependencies on the gage face hardness ratio,* with the alloyed rail exhibiting a greater susceptibility to lubrication effects. In contrast, the preliminary surface hardness results from the third experiment suggest a diminishing dependence of the unlubricated gage face wear rate on increasing hardness (figure 10). However, FHT, CrV, and bainitic CrMo were unlike the other premium rails in exhibiting no increase in gage wear resistance with increased running surface hardness. Gage face hardness data are not yet available for rails tested in the third experiment.

Head height loss rates of the low rail in the first experiment are listed in table 14. Relatively little lubrication was applied to the low rail (just enough to protect the high rail in Section 07) throughout the first experiment. Because the low rail was laid entirely upon the 1:40 cant tie plate, there was no tie plate cant effect. However, all five metallurgies did appear to exhibit a position-in-curve effect in which the center segments wore more rapidly than did the end segments. This behavior was akin to that of high rail gage face wear in the lubricated (as opposed to underlubricated) regime. The head height loss rates for the low rails were within a factor of 2 of those for the high rail in the underlubricated regime. In fact, for HiSi, FHT, and CrMo, the agreement between high rail and low rail head height loss rates was quite close.

In addition to the wear and metal flow of the rail itself, the behavior of rail weldments influences the assessment of rail adequacy. Difficulty in avoiding the formation of untempered martensite in weldments of the bainitic CrMo and the CrV rail necessitated the tempering of these weldments—the tempering procedure involved heating the weld region to 1,000° F for 20 minutes. The tempering softened some weldments sufficiently to increase their susceptibility to welded rail end batter and thus permitted the observation of rail end batter growth. Figure 11 illustrates the longitudinal profile of a battered weldment; the growth of rail end batter in both CrV and bainitic CrMo weldments is recorded in figure 12. Both weldments were in the low (inside of curve) rail, and the low rail was essentially unlubricated even in the lubricated regime. Nevertheless, the growth of rail end batter in low rail weldments increased rapidly when lubrication of the high rail ceased. After the rapid growth of rail end batter had initiated, remedial grinding failed to slow the process. Lubrication of the high rail does seem to be an effective means of slowing the development of batter even on the low rail.

------

* The ratio of premium rail gage face hardness to Std rail gage face hardness.

9 Kumar, S., and Margasahayam, R., IIT Trans - 78-1.

10 Jamison, W.E., The Wear of Railroad Freight Car Wheels and Rails, ASLE preprint 79 AM-5E-3, ASLE Annual Meeting, St. Louis, MO, April 1979.
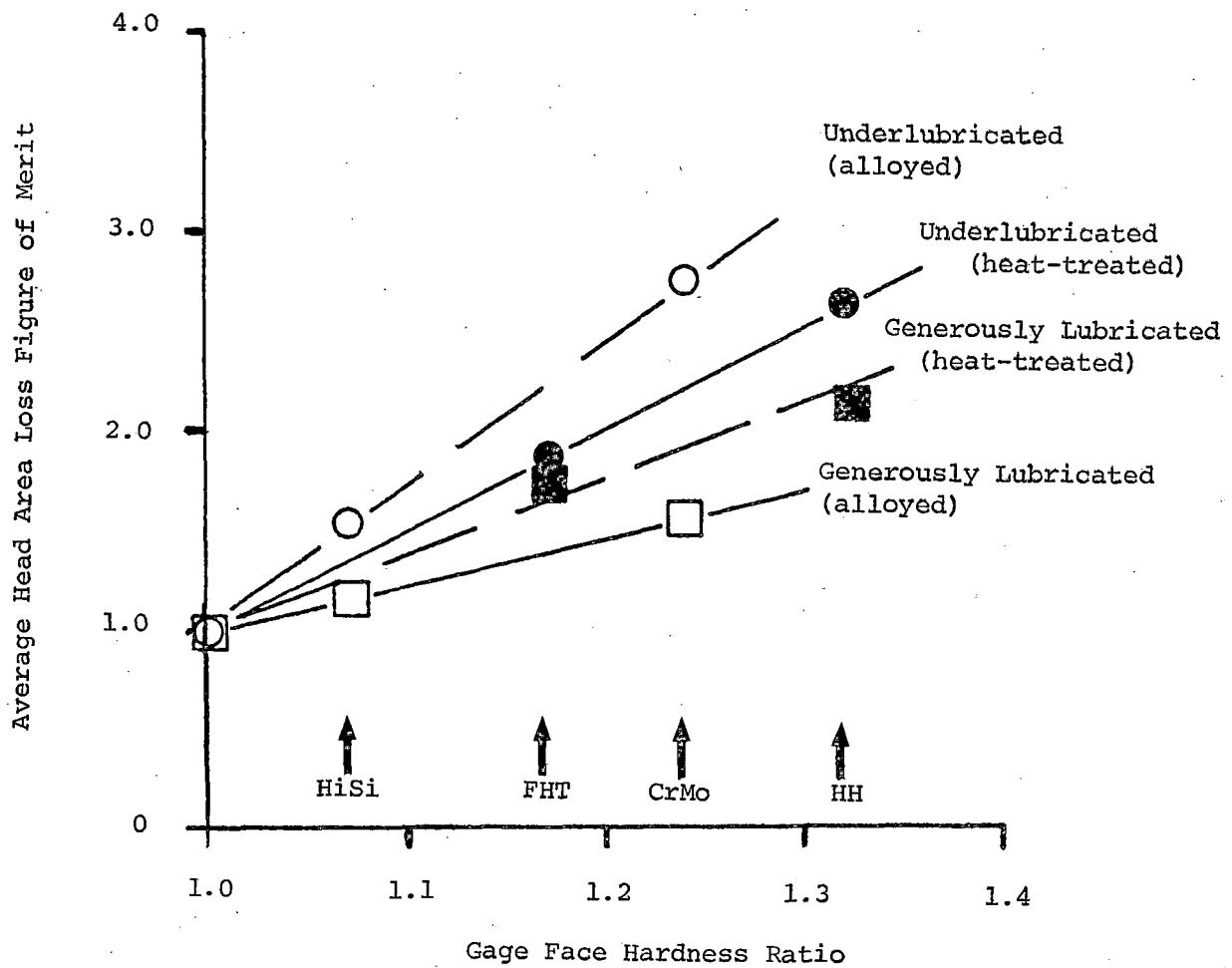
22

FIGURE 9. EFFECT OF RELATIVE GAGE FACE HARDNESS UPON
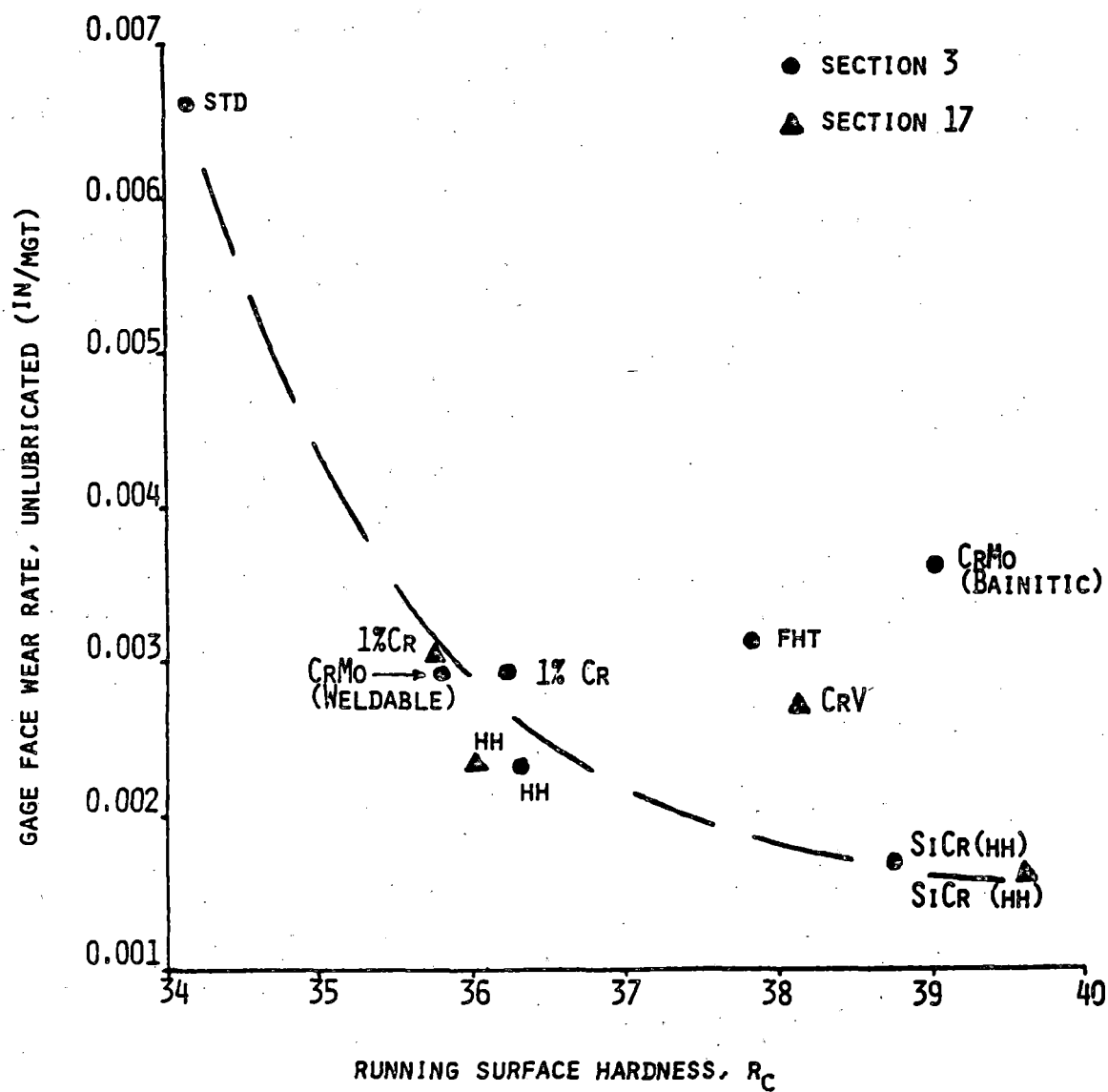HEAD AREA LOSS FIGURE OF MERIT.

FIGURE 10. RELATIONSHIP OF UNLUBRICATED GAGE FACE WEAR RATE
AND RUNNING SURFACE HARDNESS.

24

TABLE 14. LOW RAIL HEAD HEIGHT LOSS RATES FROM
THE FIRST METALLURGY EXPERIMENT.

| Section 03	Metallurgy (in/MGT)				
Segment	Std	HiSi	FHT	CrMo	HH
A	0.0014	0.0012	0.0007	0.0005	0.0004
B	0.0008	0.0010	0.0004	0.0004	0.0008
C	0.0013	0.0011	0.0007	0.0009	0.0005
D	0.0017	0.0013	0.0008	0.0008	0.0007
E	0.0017	0.0012	0.0011	0.0010	0.0008
F	0.0014	0.0015	0.0012	0.0007	0.0013
G	0.0017	0.0016	0.0009	0.0009	0.0010
H	0.0013	0.0017	0.0010	0.0006	0.0009
I	0.0013	0.0015	0.0009	0.0007	0.0008
J	0.0013	0.0010	0.0010	0.0006	0.0006
Avg	0.0014	0.0013	0.0009	0.0007	0.0008
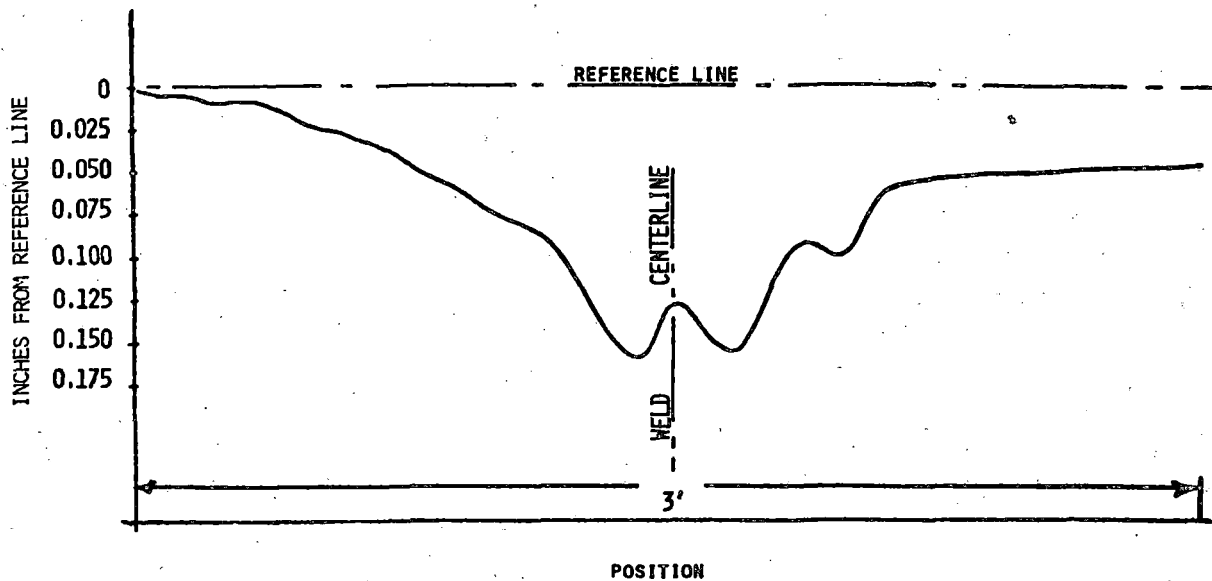
FIGURE 11   LONGITUDINAL PROFILE OF BATTERED TEMPERED CrV WELDED AFTER 33 MGT.
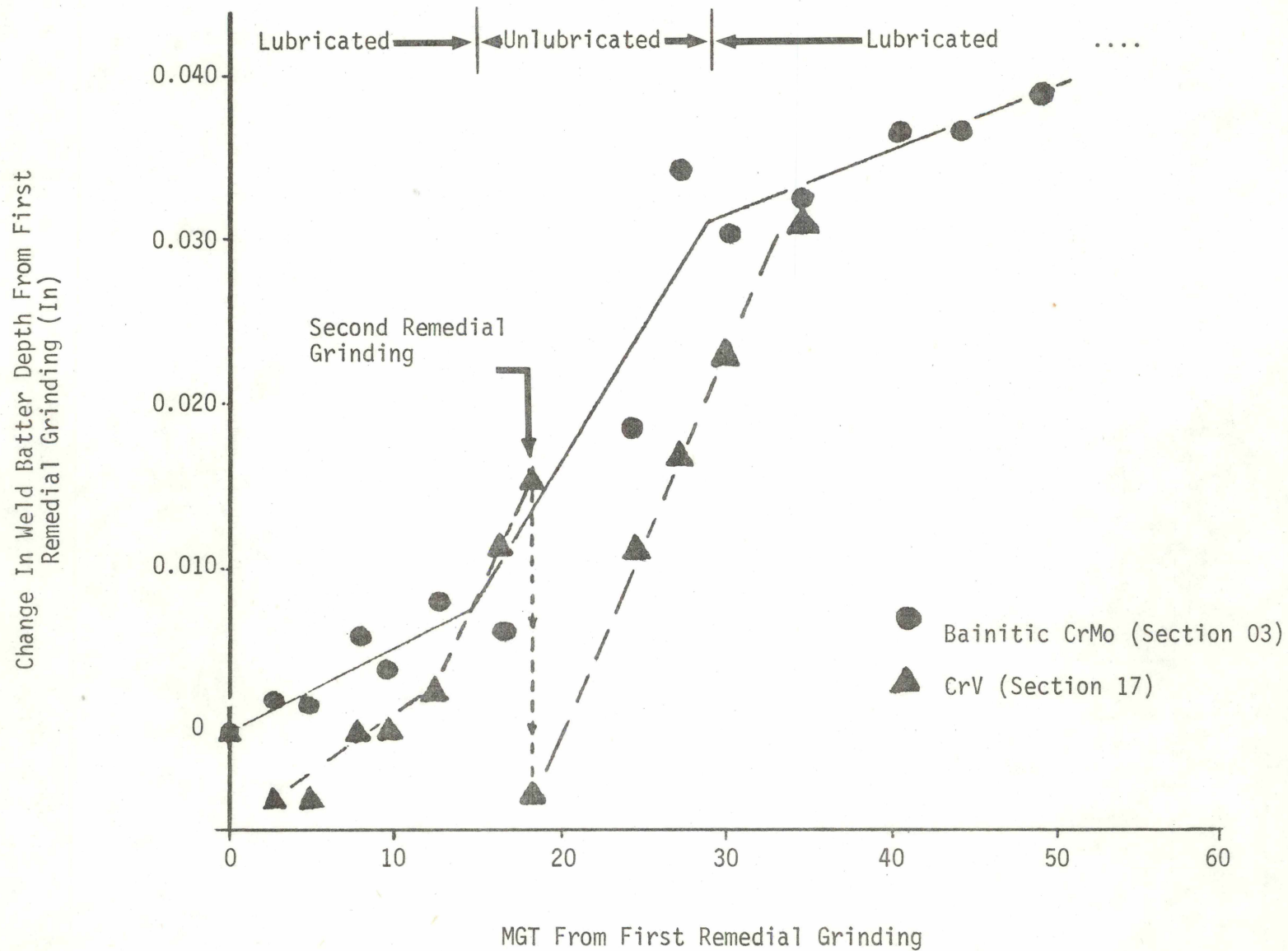
25

FIGURE 12. DEVELOPMENT OF WELDED RAIL END BATTER
IN TEMPERED WELDMENTS.

FRACTURE

Fracture of rails and weldments was a major failure mode throughout the first two experiments. However, while failure of both plant (flash butt) and field welds dominated in the first experiment, fatigue failures in the rail head became more frequent in the second experiment; table 15 summarizes the rail/weld failure occurrence.

In the first experiment, replacement field welds failed at such a high rate that the number of failures exceeded the number of field welds installed at construction. Along with rapid wear in the underlubricated regime, these weld failures necessitated the rerailing of Sections 03 and 13 at 135 MGT. In the first experiment, field weld failures occurred in the initially installed field welds as well as in the subsequently installed plug welds. However, in the second experiment, all failures were in plug welds.

In the second experiment, less wear and greater tonnage accumulation permitted the development of more fatigue-type rail head defects, but not all of the rail head defects listed in table 15 can be considered valid fatigue defects. Some of the head defects in Section 03 were at, or very near, the ends of metallurgy segments, so that their occurrence may actually have been related to mechanical joint assembly and/or maintenance and repair problems. Also, there occurred five defects in Section 13 involving several apparently "dirty" rails from a single heat of Std rail. If all these questionable defects were removed from consideration, the overall defect rates would drop to about 20/mi (of track) in Section 03 and 10/mi in Section 13.

The locations of all plant weld and head-type failures in the high rail of Section 03 in the second experiment are shown by metallurgy and tie plate cant in figure 13. Without counting those of questionable origin, Std rail had five head-type fatigue failures, yielding a rate of 44/mi (of high rail). HiSi followed with only two failures and a rate of 18/mi. HH had only one valid head-type failure. FHT had only one head-type failure, but it was at a segment end. CrMo had no head-type failures. The differences in the numbers of rail failures among premium rails probably is not significant, but Std rail exhibited a substantially higher failure rate than that of the premium rails.

HH rail had the most plant weld failures—six. Std rail had two, while CrMo and FHT rails had only one plant weld failure each within the metallurgy test section. In Section 13, Std rail had two plant weld failures, while FHT and HiSi had one plant weld failure each.

The 1:14 cant was associated with a total of nine failures, the 1:30 cant with ten failures, and the 1:40 cant with three failures. However, some of these did occur near segment ends (as can be determined in figure 13) and must be viewed as suspect. An additional consideration is the experiment design, which placed the Std, HiSi, and HH rails on the 1:14 and 1:30 cants in the midregion of the curve, while these same rails on the 1:40 cant were positioned at the ends of the curve. Thus, what appears as a tie plate cant effect may actually be a position-in-curve effect.

Although wheel/rail load measurements taken throughout Section 03 with an instrumented wheelset did not reveal any marked changes in vertical or lateral loads as a function of position-in-curve (figure 14), track geometry records

TABLE 15. TOTAL RAIL FAILURES IN METALLURGY TEST
SECTIONS 03 AND 13, BOTH RAILS.

	Plant Welds	Field Welds	Head Defects
First Experiment: (135 MGT)			
Section 03	44 (180)	44 (22)	2
Section 13	17 (64)	17 (10)	7
Second Experiment: (250 MGT)			
Section 03	10 (120)	12 (0)	15 (27/mile[1])
Section 13	4 (48)	8 (0)	7 (10/mile[2]) (30/mile[1])

( ) Figure indicates number of welds initially installed.

[1] Figure indicates defect rate at 250 MGT per mile of track.

[2] Defect rate adjusted to eliminate failures and rail length associated with "dirty" standard rail.

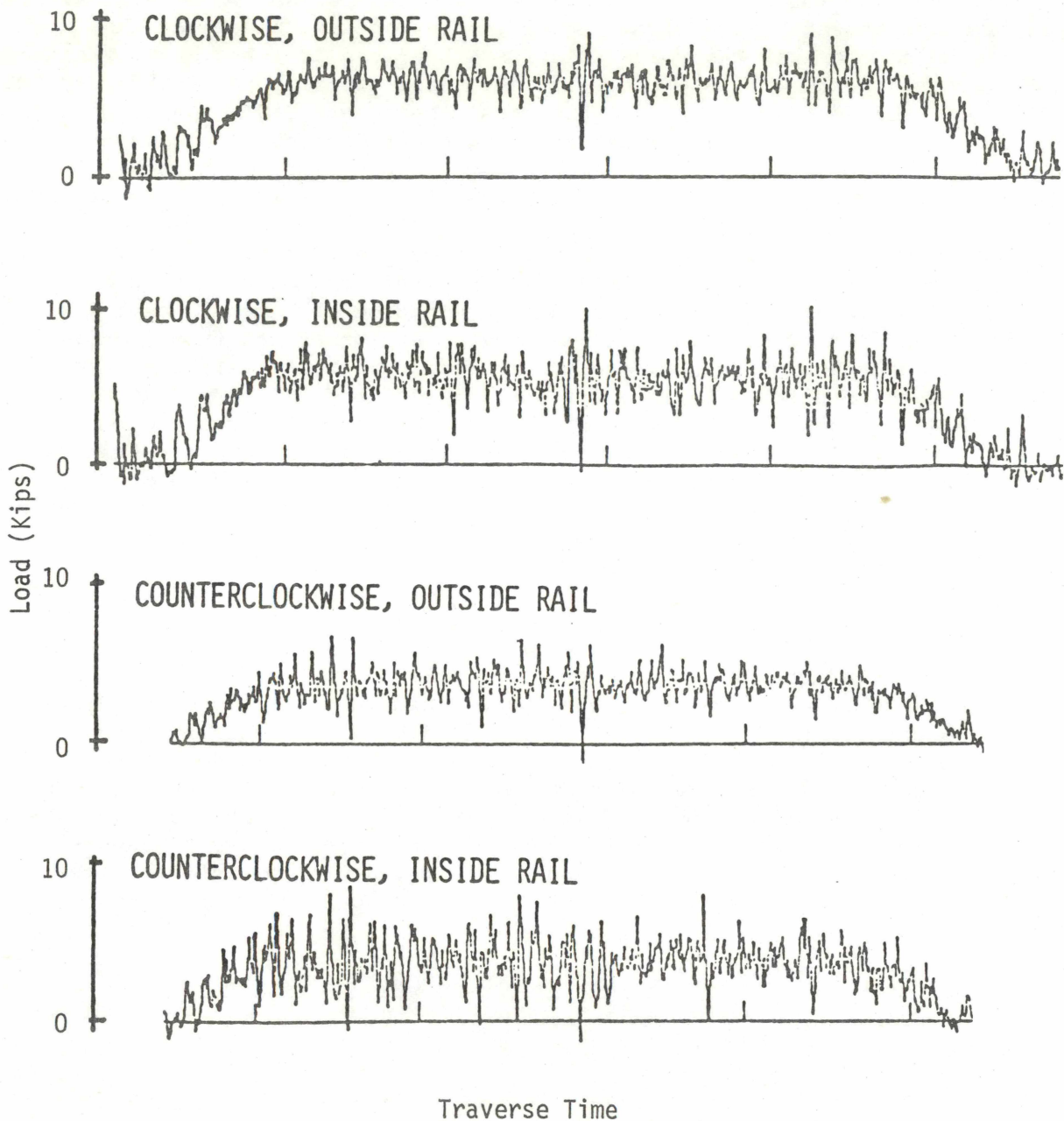FIGURE 13. LOCATIONS OF RAIL/WELD FAILURES IN SECTION 03, HIGH RAIL ONLY.

FIGURE 14. INSTRUMENTED WHEELSET MEASUREMENTS OF LATERAL WHEEL/RAIL
FORCES IN SECTION 03 AT 45 MI/H (NOMINAL), LUBRICATED.

revealed that the central portion of Section 03 suffered more loss of track alinement than did either end portion (figure 15). Similarly, Tuve[11] has observed a relationship between track geometry parameters and rail defect occurrence.

Figure 16 shows the relationship between rail failure and tonnage at FAST for Std rail in both a 5° curve (Section 03) and tangent track, as well as the rail failure line for HiSi in the 5° curve. For comparison with rail failure behavior from actual U.S. railroad service, the bands within which the Association of American Railroads (AAR)/AREA/American Iron and Steel Institute (AISI) survey[12] data fall are also plotted, as is the failure line for the WS Railroad,[13] that operated with 125-ton cars. Note that FAST experience with 100-ton cars is substantially worse than the experience of more conventional U.S. railroad operation with car weights averaging closer to 75 tons. However, the WS experience with 125-ton cars is very similar to that of FAST.

Combining the FAST rail failure information, the WS failure information, and other data from the joint AAR/AREA/AISI survey, the plot in figure 17 shows the 1 percentile failure tonnage as a function of nominal wheel load. Although it is not certain that all data sets were generated from identical types of track (same curvature, grade, tie spacing, track stiffness, etc.), if straight lines join the data sets for lighter (115 and 119 lb/yd) and heavier (136 and 140 lb/yd) rail, slopes between -1/2 (assumes 5° curvature on Santa Fe (SF) sites) and -1 (assumes tangent track on SF sites) can be obtained. These slopes are much less steep than predicted in the model developed by Zarembski[14] and exercised for tangent track. It is not clear for what failure percentile the analytical model makes its prediction, but on the basis of Zarembski's work it appears to be the 0.03 to 0.06 percentile. If this is so, the model does not fully agree with observed rail failure behavior at FAST, the WS, or SF test sites. Furthermore, the model predicts much greater shortening of rail fatigue life with increased nominal wheel load than seems to be observed in actuality. However, it should be pointed out that the analytical model specifies the nominal wheel load as "the largest static wheel load for a given mix of traffic." The actual rail failure data from the WS, the SF, and the FAST track are reported for average static wheel loads. Even if effective wheel loads were calculated for the two SF test sites by assuming that fatigue damage is accumulated in proportion to the fourth power of wheel load (in a fashion similar to that used to calculate effective tonnage[12]), the wheel loads would increase only to about 18 kips, and slopes of the lines drawn between sets of observed data would increase only slightly.

---

[11] Tuve, R.F., Application of Track Geometry Data to Track Maintenance Planning on the Southern Railway Co., presented at the 59th Annual Meeting, Transportation Research Board, January 21-25, 1980, Washington, D.C.

[12] Stone, D.H., "Track Train Dynamics Contributions to Rail Metallurgy," AREA Bulletin 673, Vol. 80, June-July 1979, pp. 528-543.

[13] Groom, J.J., "Residual Stress Determination," DOT-TSC-1426, Battelle-Columbus Laboratories, November 26, 1979 (Draft Report).

[14] Zarembski, A.M., "Effect of Rail Section and Traffic on Rail Fatigue Life," AREA Bulletin 673, Vol. 80, June-July 1979, pp. 514-527.
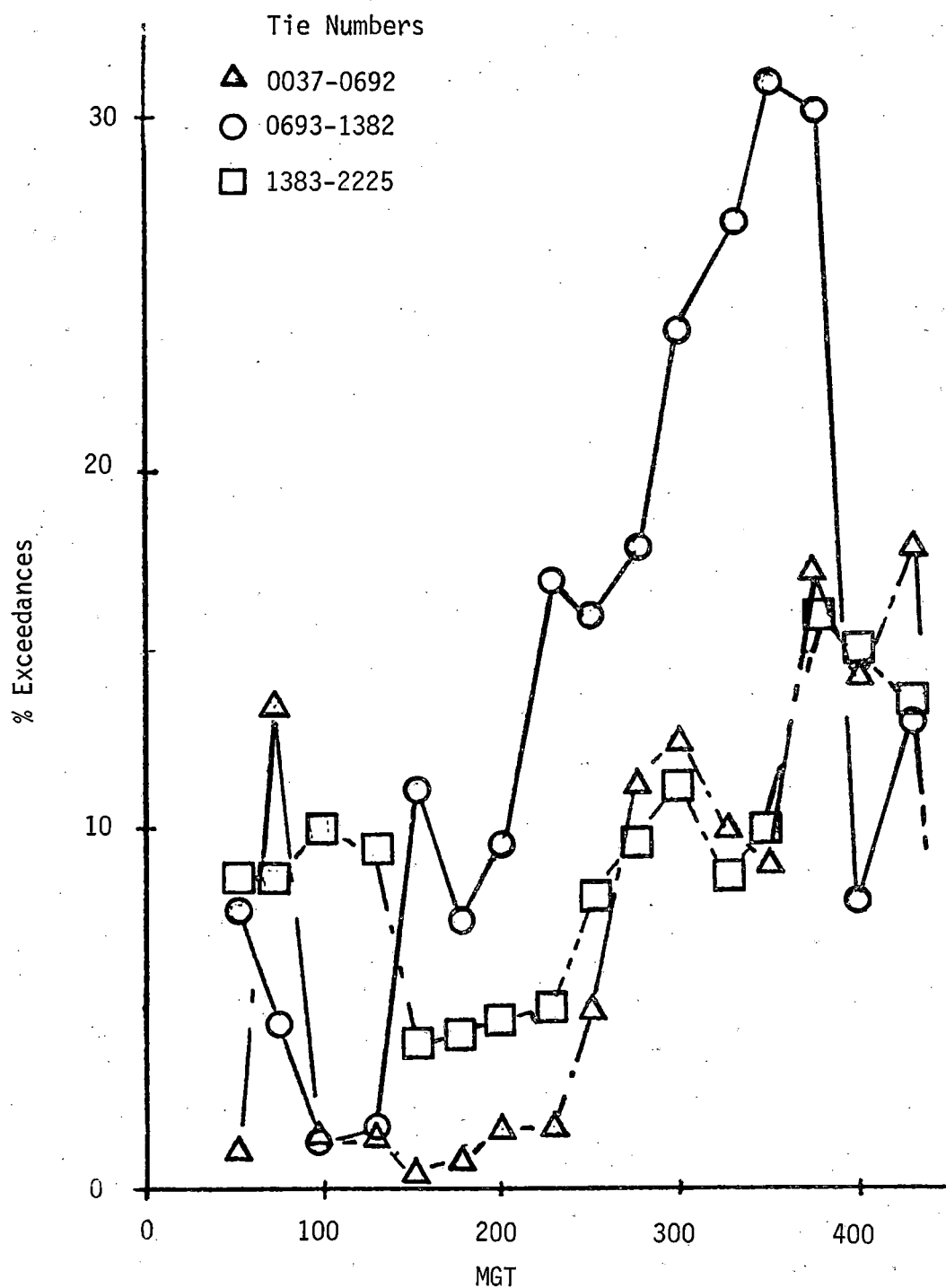
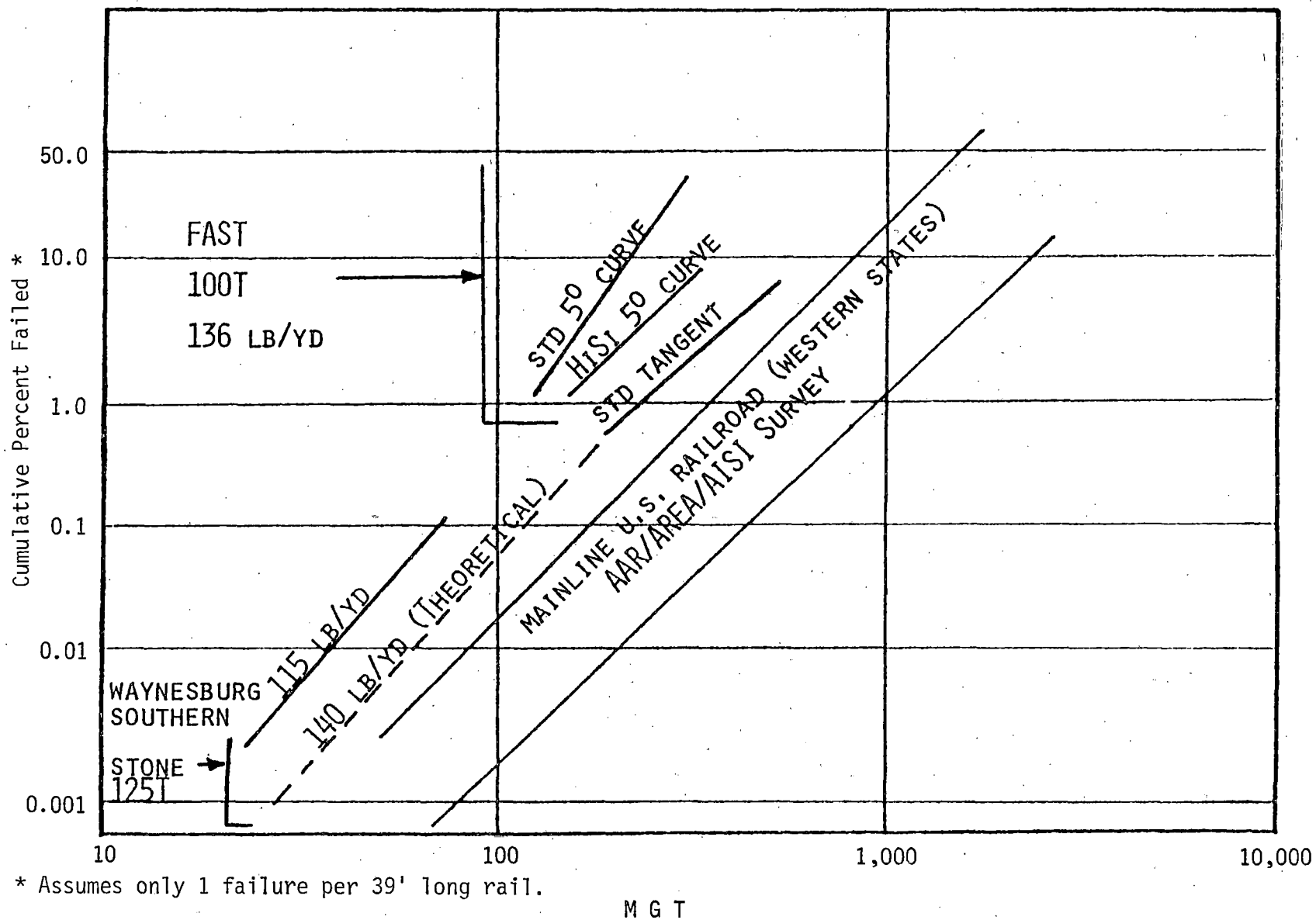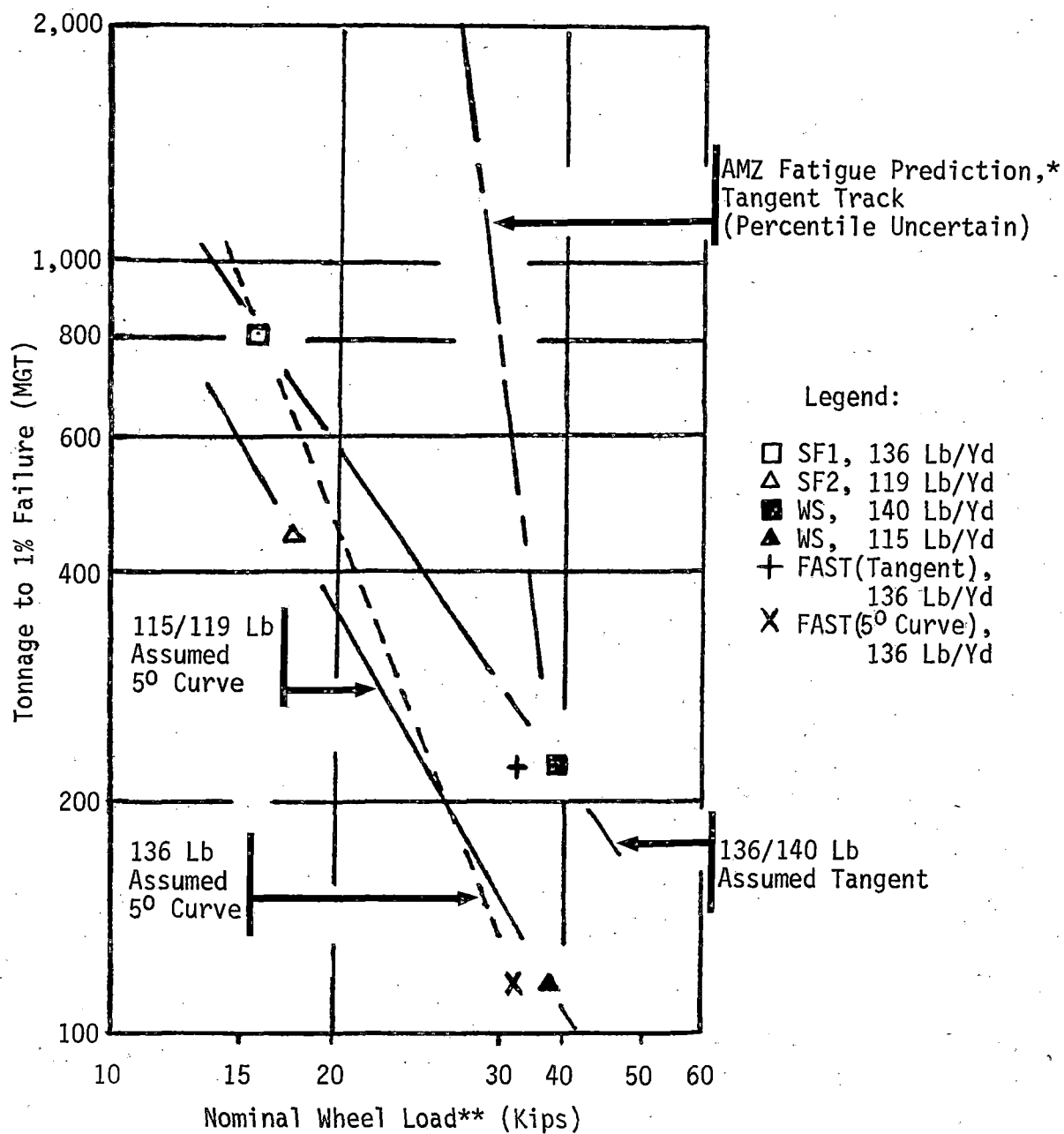FIGURE 15. ALINEMENT CHANGE AS A FUNCTION OF TRAFFIC IN SECTION 03.

FIGURE 16. WEIBULL PRESENTATION OF RAIL FAILURE DATA.

The figure plots Cumulative Percent Failed * (vertical axis, from 0.001 to 50.0) against M G T (horizontal axis, from 10 to 10,000) on log-log scale. Labeled curves include: FAST 100T 136 LB/YD; STD 50 CURVE; HiSi 50 CURVE; STD TANGENT; MAINLINE U.S. RAILROAD (WESTERN STATES); AAR/AREA/AISI SURVEY; 115 LB/YD; 140 LB/YD (THEORETICAL); WAYNESBURG SOUTHERN STONE 125T.

* Assumes only 1 failure per 39' long rail.

32

FIGURE 17.   COMPARISON OF OBSERVED 1 PERCENTILE FAILURE BEHAVIOR
WITH THEORETICAL FATIGUE ANALYSIS PREDICTION.

A typical detail fracture generated under the FAST loading environment is shown in figure 18. Reversing train direction daily (at approximately 1-MGT intervals) caused a zig-zag crack path which permitted the accurate tracking of crack growth. The crack growth pattern has been reconstructed for the detail fracture of figure 18 and is plotted in figure 19. Crack growth behavior can be used to infer the stress state that caused the crack to grow.

Two major components of the stress state are: flexural stress induced by the passing wheel, and steady stress state in the rail head (i.e., the combined effect of residual stresses induced by rail manufacture, cold working of the running surface, temperature variations, and longitudinal forces induced by train action). Work by Battelle-Columbus Laboratories[13] has shown that residual stresses locked within the rail head under the cold worked surface layers can reach levels of 15 to 20 ksi tension under FAST loading conditions. The flexural stresses can be calculated from wheel load, rail structural characteristics, and track stiffness.[15][16] However, both residual and flexural stresses cannot be determined independently from post mortem examination of a fractured rail. Nevertheless, the crack growth curve, in combination with the available knowledge of the general crack growth characteristics of rail steels,[17][18][19] can be used to define the reasonable limits of both types of stress. An approximate representation of crack growth characteristics of current U.S. standard composition rail steels can be given by the Forman expression:

$$\frac{da}{dN} = \frac{B\Delta K^n}{[(1-R)K_c - \Delta K]}$$

where:

$B = 3 \times 10^{-9}$ in/cycle

$n = 3.32$

$K_c = 50$ ksi $\sqrt{in}$

-----

[13] Op. cit.

[15] McConnell, D.P., and Perlman, A.B., "An Investigation of the Structural Limitations of Railroad Track," DOT-TSC-1575, Tufts University, June 1979 (Interim Draft Report).

[16] Talbot, A.N. (Chairman), "Stresses In Railroad Track," Reports 1-7, AREA Bulletin, Volumes 19, 21, 24, 26, 31, 35, and 42.

[17] Fowler, G.J., and Tetelman, A.S., "The Effect of Grain Boundary Ferrite on Fatigue Crack Propagation In Pearlitic Rail Steels," Rail Steels - Developments, Processing, and Use, STP 644, American Society for Testing and Materials, Philadelphia, PA, 1978, pp 363-386.

[18] Fedderson, C.E., and Broek, D., "Fatigue Crack Propagation In Rail Steels," Rail Steels - Developments, Processing, and Use, STP 644, American Society for Testing and Materials, Philadelphia, PA, 1978, pp 414-429.

[19] Barsom, J.M., and Imhof, E.J., "Fatigue and Fracture Behavior of Carbon-Steel Rails," STP 644, American Society for Testing and Materials, Philadelphia, PA, 1978, pp 387-413.

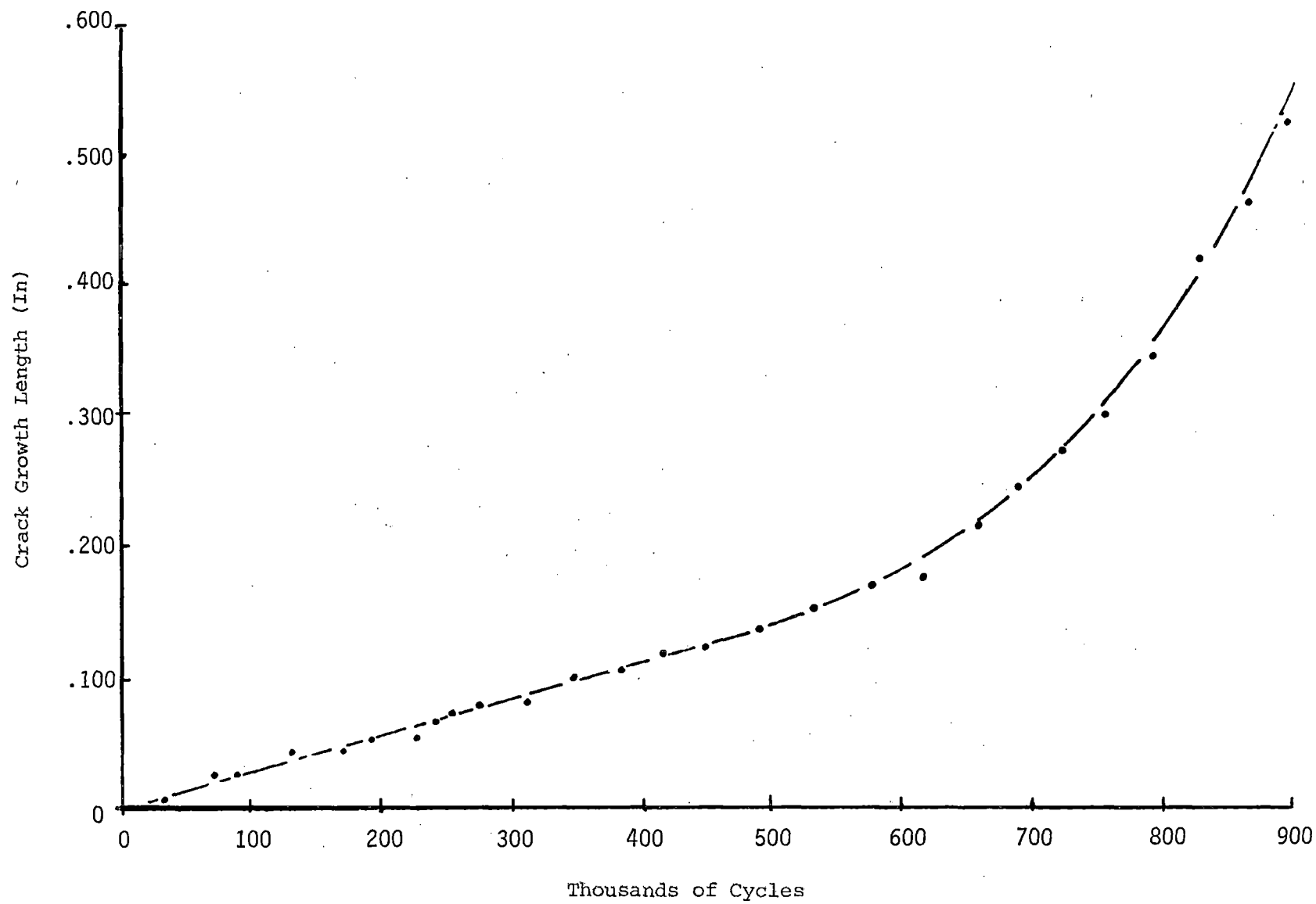FIGURE 18.   DETAIL FRACTURE FROM SHELL, 115 LB/YD RAIL, SECTION 13.

FIGURE 19. CRACK GROWTH LENGTH VS. NUMBER OF WHEEL CYCLES.

$$\Delta K = 1.13 \ \Delta\sigma \ \sqrt{a}$$

$\Delta\sigma =$ the varying stress range

$a =$ the crack radius

The integrated Forman expression can be used to generate a family of crack growth curves for comparison with the observed growth curve. This is illustrated in figure 20 for a variety of assumed wheel loads on 115 lb/yd rail supported on a track structure with a modulus of 1,500 lb/in^2. Figure 21 presents estimates of the best effective wheel load/residual stress levels from the family of curves. If a residual stress level of 20 to 25 ksi is considered reasonable, the effective vertical wheel load would be in the range of 41 to 46 kips--roughly 25% to 40% more than the true static vertical wheel load. This apparent augmentation of the vertical wheel load agrees with that predicted by the analysis of McConnell and Perlman[15] for the lateral flanging forces of 8 to 10 kips observed in Section 13.

The initial crack path for the fracture under consideration was inclined at an angle of about 30° to the vertical plane (figure 22). After a few tenths of an inch propagation, the crack ran in an essentially vertical path, which--with the zig-zag progression of the crack path--suggests that shear stresses also influenced initiation and growth of the crack by causing the principal stresses to rotate.

The shell surface running horizontally under the gage corner of the rail was also zig-zagged; a vertical crack that developed from one of the valleys of the shell crack is shown in figure 23. The shell crack and the origin of the detail (vertical) crack occurred 12 mm beneath the surface. Figure 24 shows where the fatigue crack originated relative to the peak hardness caused by cold working. Figure 25 is a hardness map of a transverse cross section of the rail 1-1/2" back from the detail fracture. An intrusion of softer metal (200 to 229 Vickers Hardness Number (VHN)) occurred at about the level of the shell and the vertical crack initiated at the lower boundary of this intrusion. The level of the shell was well below the region (0.10 to 0.15") where maximum octahedral shear stresses would be expected to occur under 33-kip wheel loads.[20] The maximum hardness does occur at this depth. The observations of Gervais and McQueen[21] are consistent with these findings. The model of shell and detail fracture proposed by Ghonem[22] is supported by observations at FAST, except that FAST information does not confirm that a shell must initiate at the lower edge of the gage face.

-----

[15] Op. cit.

[20] Johns, T.G.; Davis, K.B.; McGuire, P.M.; Sampath, S.G.; and Rybicki, E.F., Engineering Analysis of Stresses in Railroad Rails: Phase I, DOT-TSC-1038, June 1977.

[21] Gervais, E., and McQueen, H.J., Journal of the Iron and Steel Institute, March 1969, pp. 189-198.

[22] Ghonem, H., and Pak, W., "Study of Fatigue Characteristics of Rail Steel," Final Report Track/Train Dynamics Program, Phase III, October 1, 1978 - May 15, 1979.
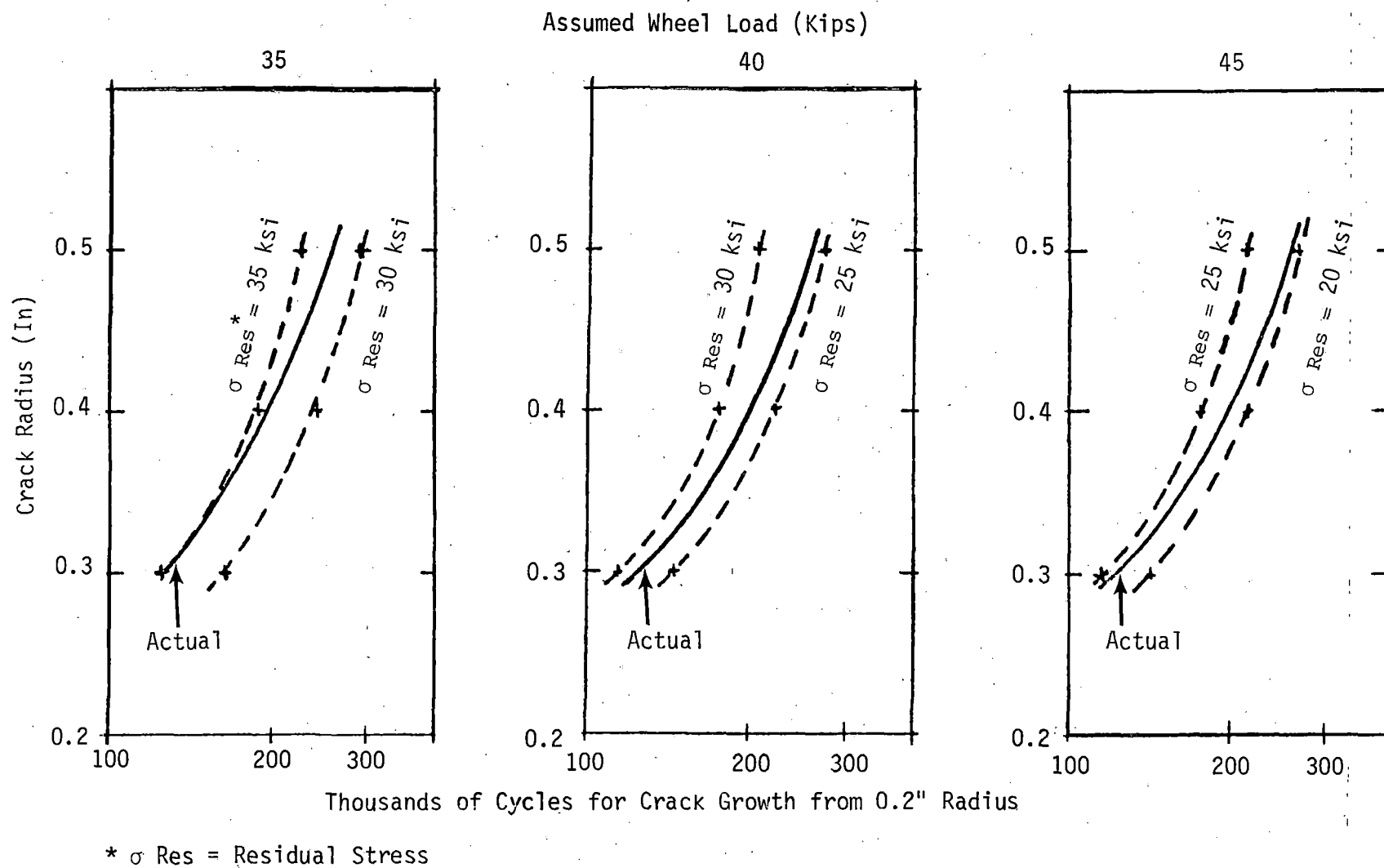
Assumed Wheel Load (Kips)

FIGURE 20. COMPARISON OF ACTUAL CRACK GROWTH WITH FAMILIES
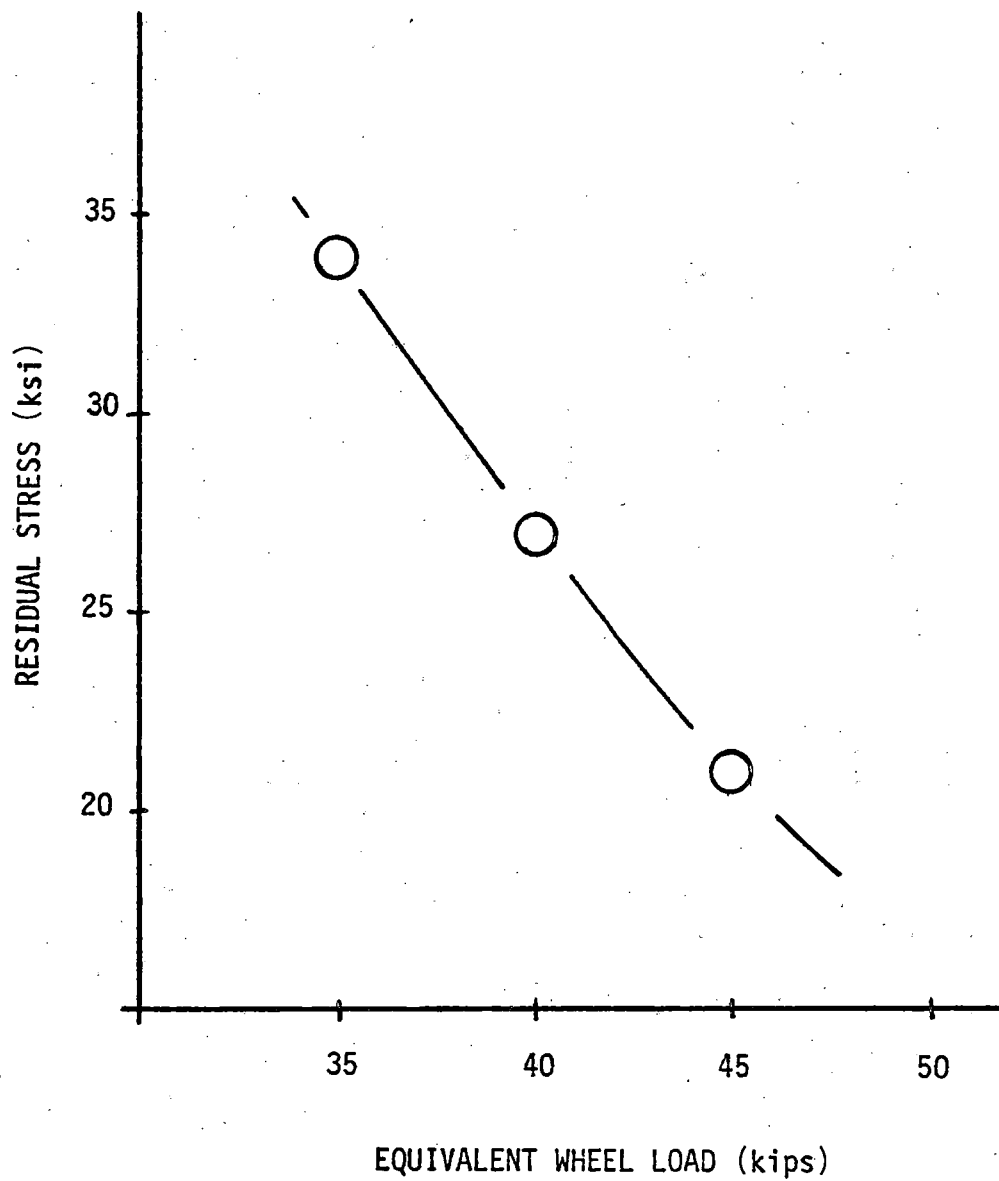OF CALCULATED GROWTH CURVES.

* σ Res = Residual Stress

FIGURE 21. WHEEL LOAD/RESIDUAL STRESS COMBINATIONS
FOR OBSERVED CRACK GROWTH.

FIGURE 22.   INCLINATION OF CRACK PATH.
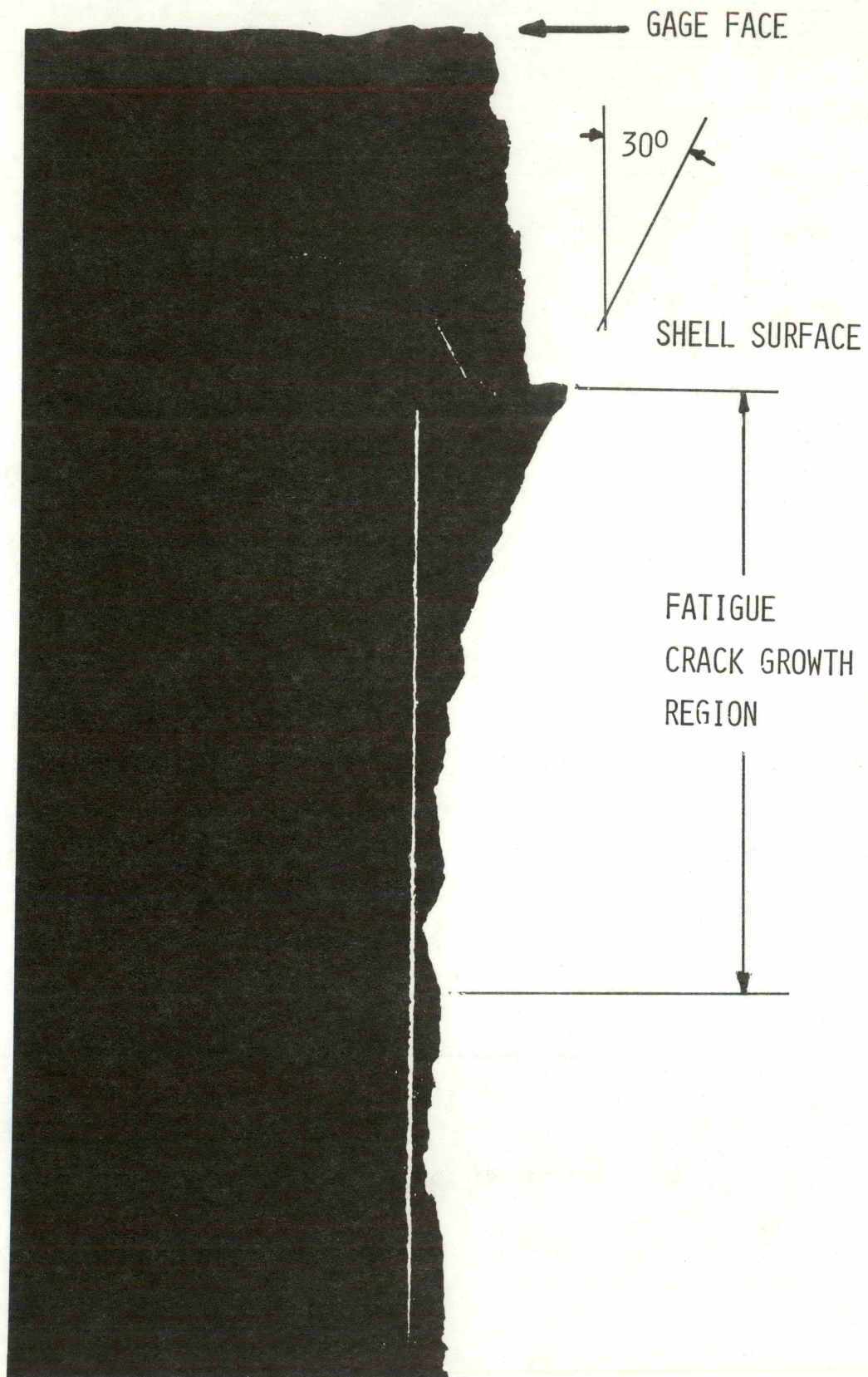
GROWTH OF VERTICAL
CRACK FROM VALLEY
ON SHELL CRACK
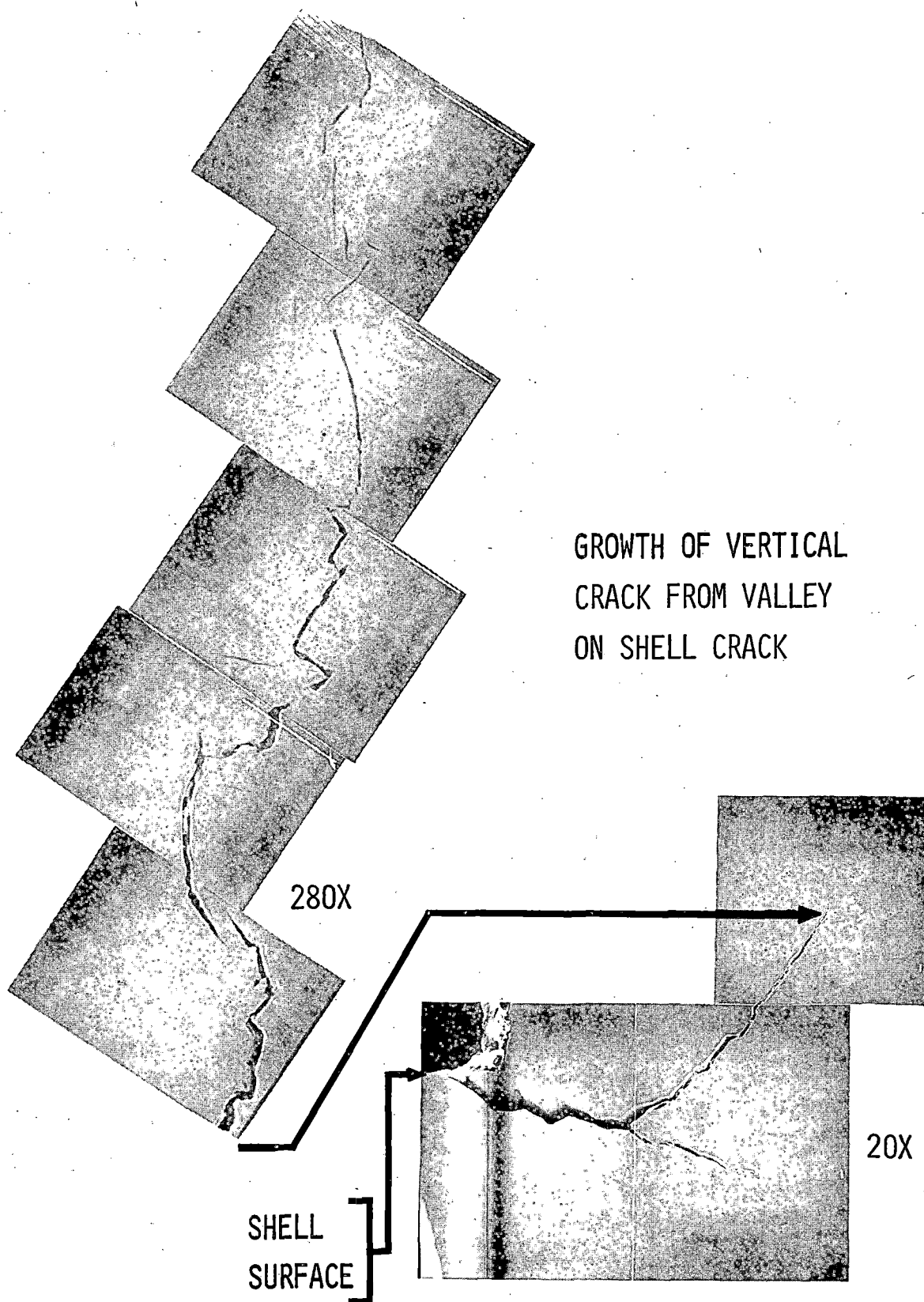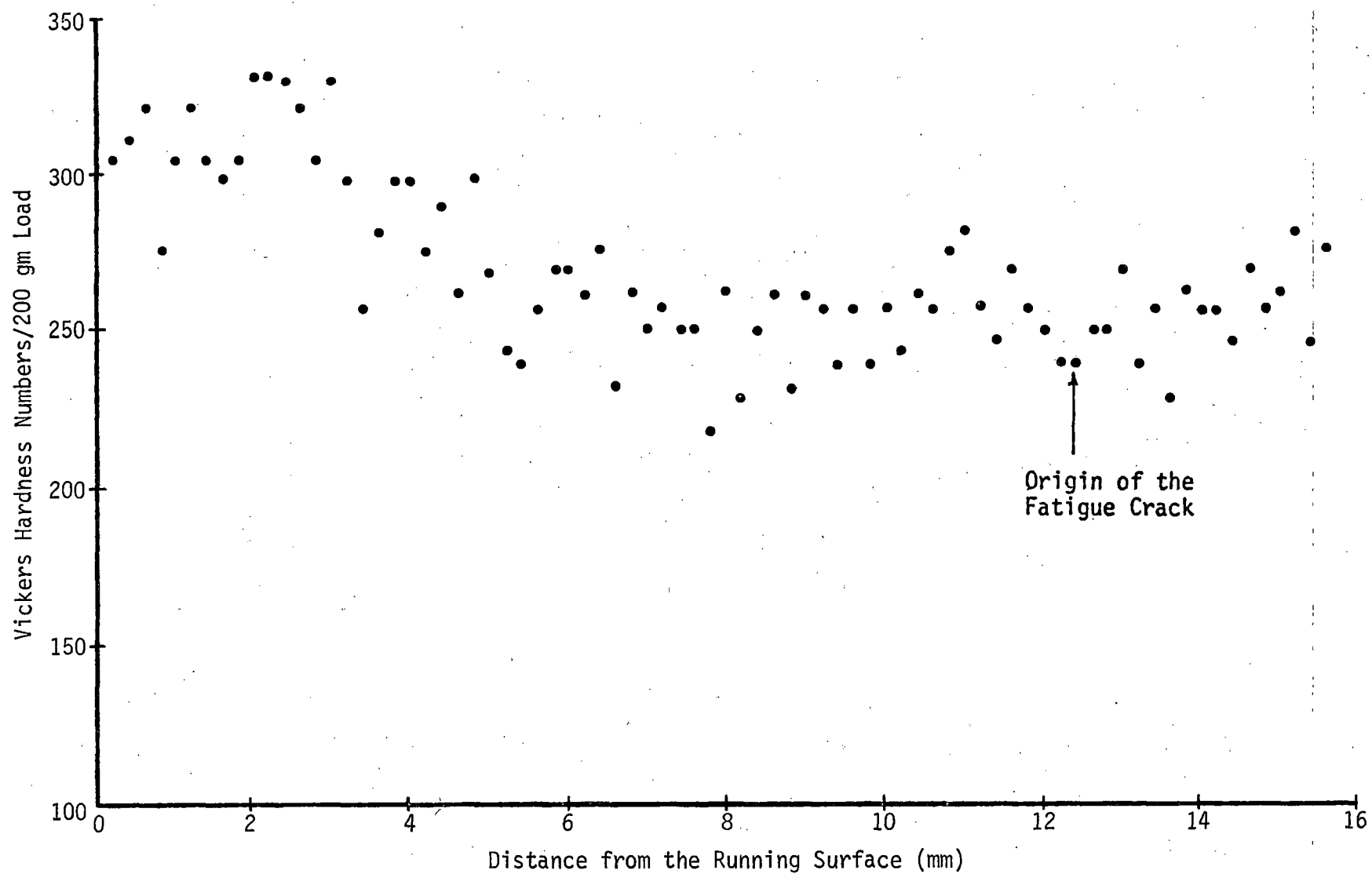
280X

20X

SHELL
SURFACE

FIGURE 23. GROWTH OF A VERTICAL CRACK FROM A VALLEY ON A SHELL CRACK.

41

FIGURE 24. VHN VS. DISTANCE FROM THE RUNNING SURFACE
ON THE TRANSVERSE PLANE.

NOT TO SCALE

>260　　　　　　>260

>260

230-259　　　　　　230-259

200-229

ORIGIN OF
TD

200-
229

200-229　　200-229　　230-259

230-259　　230-259

230-
259　　200-229

230-
259

>260

230-259

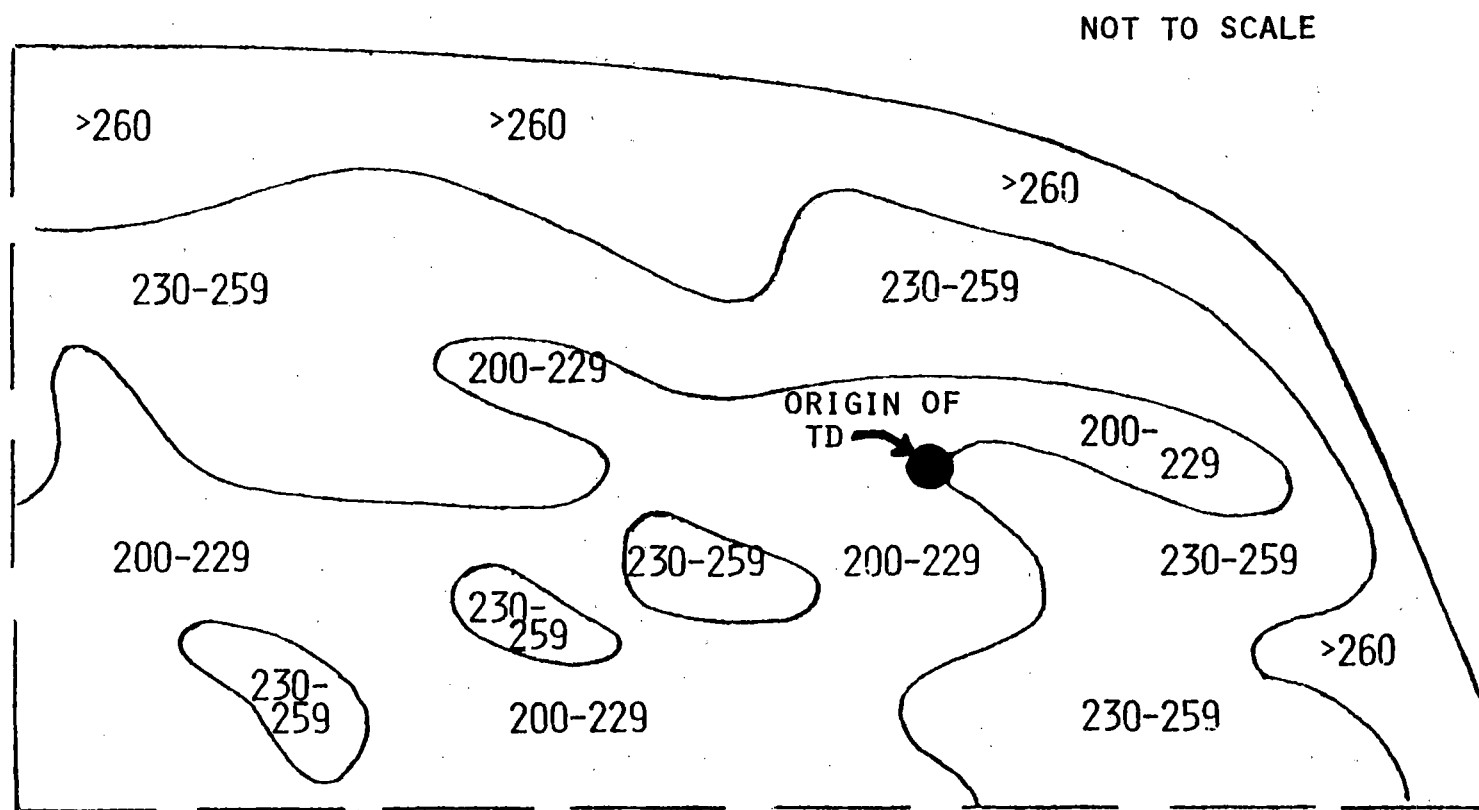NUMBERS ARE VICKERS HARDNESS NUMBER (200G)

FIGURE 25.　HARDNESS MAP OF RAIL CONTAINING A TRANSVERSE DEFECT.

CONCLUDING REMARKS

The rail wear and failure behavior at FAST have been described and comparisons have been drawn with comparable information from other railroad operations. An important metallurgy/lubrication interaction has been shown to exist. A strong contribution of equivalent carbon content to rail wear has been suggested. Rail failure at FAST has been found to be consistent with that of conventional U.S. railroad operation when allowances are made for the differences in wheel loads. The growth of a fatigue defect in a rail head has been shown to agree well with predictions made from a linear elastic fracture mechanics model in which an augment for lateral loading is incorporated.

REFERENCES

1. Clayton, P., "The Relationships Between Wear Behavior and Basic Material Properties for Pearlitic Steels," Wear of Materials 1979, American Society of Mechanical Engineers, New York, N.Y., pp 35-44.

2. Rougas, M., 1975 Technical Proceedings of the 12th Annual Railroad Engineering Conference, Report No. FRA-OR&D-76-243, October 1975, pp 41-44.

3. Hay, W.W.; Reinschmidt, A.J.; Bakas, P.T.; and Schuch, P.M., Economic Evaluation of Special Metallurgy Rails, Report No. ENG-76-2002, University of Illinois at Urbana-Champaign, Urbana, IL, January, 1976, NTIS #PB 252 024.

4. Stone, D.H., Comparison of Rail Behavior with 125-Ton and 100-Ton Cars, Report No. R-405, Association of American Railroads, Chicago, IL, January, 1980.

5. Curcio, P.; Marich, S.; and Nisich, G., "Performance of High Strength Rails in Track," Paper I.10, Heavy Haul Railways Conference, Perth, Western Australia, September, 1978.

6. Jamison, W.E., Wear of Steel in Combined Rolling and Sliding, ASME/ASLE Lubrication Conference, San Francisco, California, August 18-21, 1980.

7. Marich, S., and Curcio, P., MRL Report/083/76/015, Broken Hill Proprietary Co., Melbourne, Australia.

8. Babb, A.S., and Lee, J., Fourth International Wheelset Congress, July 1972, pp 16-30.

9. Kumar, S., and Margasahayam, R., IIT Trans - 78-1.

10. Jamison, W.E., The Wear of Railroad Freight Car Wheels and Rails, ASLE preprint 79 AM-5E-3 ASLE Annual Meeting, St. Louis, April 1979.

11. Tuve, R.F., Application of Track Geometry Data to Track Maintenance Planning on the Southern Railway Co., Presented at the 59th Annual Meeting, Transportation Research Board, January 21-25, 1980, Washington, D.C.

12. Stone, D.H., Track Train Dynamics Contributions to Rail Metallurgy, AREA Bulletin 673, Vol. 80, pp 528-543, June-July 1979.

13. Groom, J.J., Residual Stress Determination, DOT-TSC-1426, Battelle-Columbus Laboratories, November 26, 1979 (Draft Report).

14. Zarembski, A.M., Effect of Rail Section and Traffic on Rail Fatigue Life, AREA Bulletin 673, Vol. 80, pp 514-527, June-July 1979.

15. McConnell, D.P., and Perlman, A.B., An Investigation of the Structural Limitations of Railroad Track, DOT-TSC-1575, Tufts University, June 1979 (Interim Draft Report).

16. Talbot, A.N. (Chairman), Stress in Railroad Track, Reports 1-7, AREA Bulletin, Vol. 19, 21, 24, 26, 31, 35, 42.

17. Fowler, G.J., and Tetelman, A.S., "The Effect of Grain Boundary Ferrite on Fatigue Crack Propagation in Pearlitic Rail Steels," Rail Steels - Developments, Processing, and Use, (STP) 644, American Society for Testing and Materials, Philadelphia, PA, 1978, pp 363-386.

18. Fedderson, C.E., and Broek, D., "Fatigue Crack Propagation in Rail Steels," Rail Steels - Developments, Processing, and Use, STP 644, American Society for Testing and Materials, Philadelphia, PA, 1978, pp 414-429.

19. Barsom, J.M., and Imhof, E.J., "Fatigue and Fracture Behavior of Carbon-Steel Rails," STP 644, American Society for Testing and Materials, Philadelphia, PA, 1978, pp 387-413.

20. Johns, T.G.; Davis, K.B.; McGuire, P.M.; Sampath, S.G.; and Rybicki, E.F.; Engineering Analysis of Stresses in Railroad Rails:Phase I, DOT-TSC-1038, June 1977.

21. Gervais, E., and McQueen, H.J., Journal of the Iron and Steel Institute, pp 189-198, March 1969.

22. Ghonem, H., and Pak, W., Study of Fatigue Characteristics of Rail Steel, Final Report Track/Train Dynamics Program, Phase III, October 1, 1978 - May 15, 1979.

A Perspective Review of Rail Behavior at the
Facility for Accelerated Service Testing, 1981
US DOT, FRA (TTC)